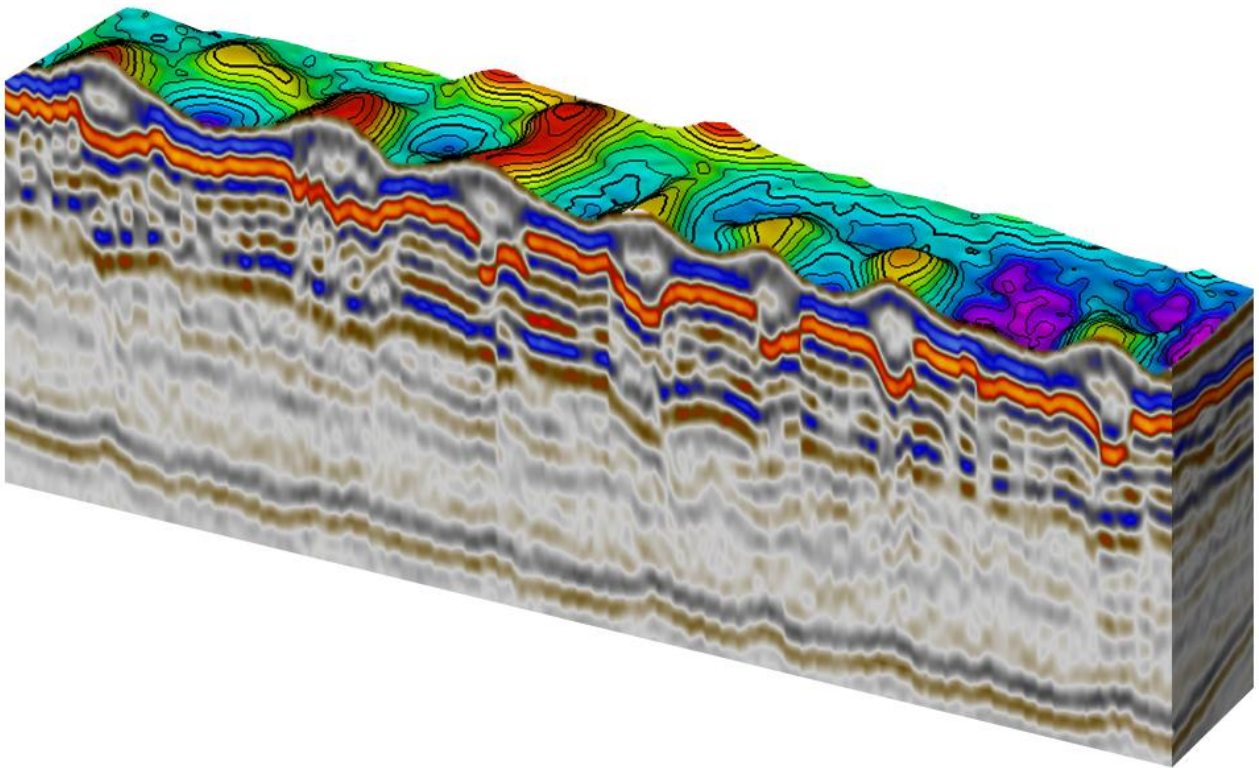




Universiteit Utrecht



Subsurface sediment remobilization and polygonal faulting in the northern Dutch offshore



Master Thesis

P.J. Stroosma
March-September 2012

Supervisors: M. van den Boogaard (EBN)
H.L.J.G. Hoetz (EBN)
Dr. J.H.P. de Bresser (UU)

Cover page image: *Mounded features observed in Dutch offshore block E-07 and their relation with underlying polygonal faulting as seen on seismic data (fig.44) (vertical exaggeration. 7,5).*

Abstract

In this research project 3D seismic data are examined for the characterization of fluid flow expressions in Lower Tertiary sediments of the northern Dutch offshore. The study area is located in quadrants A-G, with focus on the D- and western E- quadrants. The availability of new 3D seismic data in this region allowed accurate mapping and quantification of the fluid flow features present. These features might represent migration pathways for ascending hydrocarbons and can potentially be related to dry wells drilled in the study area. In total, a number of 135 mounded structures have been recognized on the Mid Miocene Unconformity. The focus of this research is to investigate the relationship between these mounded structures and the underlying polygonal fault system present in the Paleogene sediments. This relationship is examined via quantitative analysis on the polygonal faults, which include azimuth, throw and fault trace length measurements. Results show that areas where fault throw is largest, mounded structures are generally present. Furthermore, a positive relation exists between the mound height and magnitude of the underlying fault throw. These relationships combined with the characteristics found on 3D seismic data, indicate that the mounds most likely originate from remobilized sediments. Fluids dewatering from the underlying polygonal faulted sequence resulted in the entrainment and expulsion of these sediments on the paleo seafloor. The lithology of the mounds however, is uncertain as no wells have been drilled through these structures. Finally this research discusses the implications for the petroleum industry, as the observed fluid flow features are known migration pathways and might represent drilling hazards.

Keywords:

Polygonal faulting, subsurface sediment remobilization, mounds, fluid flow

Table of contents

Abstract		i
Table of Contents		iii
1.	Introduction	1
1.1	Objective	1
1.2	Study area	2
1.2.1	Geological setting – Main structural elements	3
1.2.2	Geological setting – Lithostratigraphy	4
1.2.3	Geological history	8
2.	Background	10
2.1	Polygonal fault systems	10
2.2	Subsurface sediment remobilization	19
3.	Data & Methods	25
	<i>Data</i>	
3.1	Seismic data	25
3.2	Well data	26
	<i>Methods</i>	
3.3	Interpretation and visualization tool (Petrel Software)	
3.3.1	Constructing maps	27
3.3.2	Time-depth conversion	28
3.4	Measurements for quantitative analysis	
3.4.1	Measurements on mounded structures	28
3.4.2	Measurements on polygonal faults	28
4.	Observations & Results	
4.1	Mounded structures	31
4.1.1	Seismic character	34
4.1.2	Geometry	36
4.2	Polygonal faulting	37
4.2.1	Seismic character	38
4.3	Quantitative analysis on polygonal faults and mounded structures	
4.3.1	Polygonal fault measurements	40
4.3.2	Relationship between polygonal faults and mounded structures	47

5.	Discussion	
	5.1 Distribution of the mounded structures	48
	5.2 Mounds: Lithology and origin	49
	5.3 Implications for the petroleum industry	54
6.	Conclusion	55
7.	Recommendations	56
8.	Acknowledgements	56
9.	Appendix	
	Appendix A: Additional observations	57
	Appendix B: Mound measurements and maps	66
	Appendix C: Quantitative measurements on polygonal faults	68
	Appendix D: Other maps	
	-Tectonostratigraphic map	71
	-Magnetic anomaly	72
10.	References	73

1. Introduction

Geological fluid flow processes are increasingly being recognized as important dynamic components in sedimentary basins. Especially in the last few decades, fluid migration pathways, and associated surface escape structures, gained increased attention because of their importance for the petroleum industry (Berndt, 2005; Cartwright et al, 2007; Loseth et al, 2009; Huuse et al, 2010). These structures are characterized by vertical fluid flow through otherwise impermeable sediments by breaching the sealing sequence, and thereby affecting the sealing capacity of the layer (Gay et al, 2004). Furthermore these features are often related to hydrocarbon migration and therefore could be indicative for deeper hydrocarbon bearing reservoirs or represent drilling hazards.

Surface fluid flow expressions such as mud volcanoes, are well known features onshore and have been studied for over 100 years (Kopf, 2002). However, in the subsurface as well as offshore they have rarely been recognized until the widespread availability of 3D seismic data (Hansen et al, 2005; Huuse et al, 2010). Numerous fluid escape features have been recognized and comprise surface relief features e.g. pockmarks, which represent circular depressions, or mud- and sand volcanoes and carbonate build-ups, representing a positive relief (Dahlgren and Lindberg, 2005; Hansen et al, 2005; Hurst et al, 2006; Andresen et al, 2008, 2009, 2010). On 3D seismic data the underlying migration pathways and sources can now be visualized, such as sediment intrusions, pipe structures and gas chimneys (Schroot et al, 2003; Cartwright et al, 2007; Loseth et al, 2009; Husthoft et al, 2010). Other features related to fluid escape are polygonal fault systems (Hansen et al, 2004; Gay et al, 2004; Cartwright, 1994; Ostanin et al, 2012). These systems represent laterally extensive networks of small extensional faults, show a distinct polygonal geometry in planview and are related to sediment compaction and associated fluid expulsion in very fine grained sediments (Cartwright, 1994, 2011).

1.1 Objective

Fluid flow expressions continue to be recognized in sedimentary basins worldwide, even in already well explored areas as the North Sea (Andresen, 2008, 2009, 2010; Svendsen et al, 2010; Kilhams et al, 2011). Recently a relationship has been identified between the polygonal fault system (Cartwright et al, 1994) and sandstone intrusions found in Paleogene sediments of the North Sea, in which the intrusions exploit the polygonal faults as migration pathways (Murphy and Wood, 2011). The original aim of this research was to investigate the presence of intrusive sandstones in the northern Dutch offshore. However, these intrusions have not been identified on 3D seismic data, but other possible fluid escape features have been found.

Therefore, the revised objective is to gain a better understanding of the geological fluid flow escape features present in the northern Dutch offshore. This research focuses on the observed positive relief features e.g. mounded structures found on the Mid Miocene Unconformity (~700-800 m depth) in the Dutch D- and E quadrants, as well as the underlying Paleogene polygonal fault system. Furthermore the possible implications of these features for the petroleum industry are briefly discussed.

This study focuses on two specific questions.

1. What is the origin and composition of the mounded structures, and which factors are related to their distribution?
2. Is there a relationship between the polygonal fault system and the mounded structures, as the mounds potentially represent remobilized sediment features?

In order to answer these questions, the following actions have been taken:

1. An inventarisation of the available literature on polygonal fault systems and subsurface sediment remobilization.
2. Characterization of potential fluid escape features via 3D seismic data analysis in Paleogene sediments of the study area.
3. Attempt to find, and explore a relationship between the polygonal fault system and the mounded structures via a quantitative analysis. This analysis comprises azimuth, throw and fault trace length measurements on the polygonal faults.

The outline of this report is as follows: The description of the study area is given in section 1.2 and comprises the structural elements, lithostratigraphy and the geological history. Background information on polygonal fault systems and subsurface sediment remobilization is given in chapter 2. Information on data and methods can be found in chapter 3. The observations on seismic data as well as the results of the quantitative analysis are described in chapter 4. In chapter 5 the observations are interpreted and discussed relating to the distribution, lithology and origin of the mounded structures. Furthermore the possible implications for the petroleum industry are being discussed. Chapter 6 is composed of the conclusions of this research. Chapter 7 comprises recommendations for future research. Chapter 8 forms the Appendix and consists of additional observations done in this research, which have not been investigated in depth due to time restrictions. These observations have been identified and documented. Furthermore the measurements on the mounded structures as well as the polygonal faults have been supplied.

1.2 Study Area

The study area comprises the blocks A- to G in the northern Dutch offshore, with a focus on the D quadrants (D-09, D-12, D-15, D-18) and E-quadrants (E-01, E-02, E-04, E-07, E-10, E-13, E-16, E-17). The study area is located in the North Sea basin and is bounded by the United Kingdom in the west and Germany in the northeast (fig.1).

This research focuses on the Early Tertiary sediments of the northern Dutch offshore. These sediments have been buried rapidly during Late Tertiary time and might therefore be susceptible for generating fluid escape features. The focus area has been selected based on the newly available 3D seismic data, combined with the distribution of the mounded structures observed in this research. Therefore the focus area has been investigated every seismic line, whereas the other parts of the northern Dutch offshore have only been investigated every ~10 seismic lines.

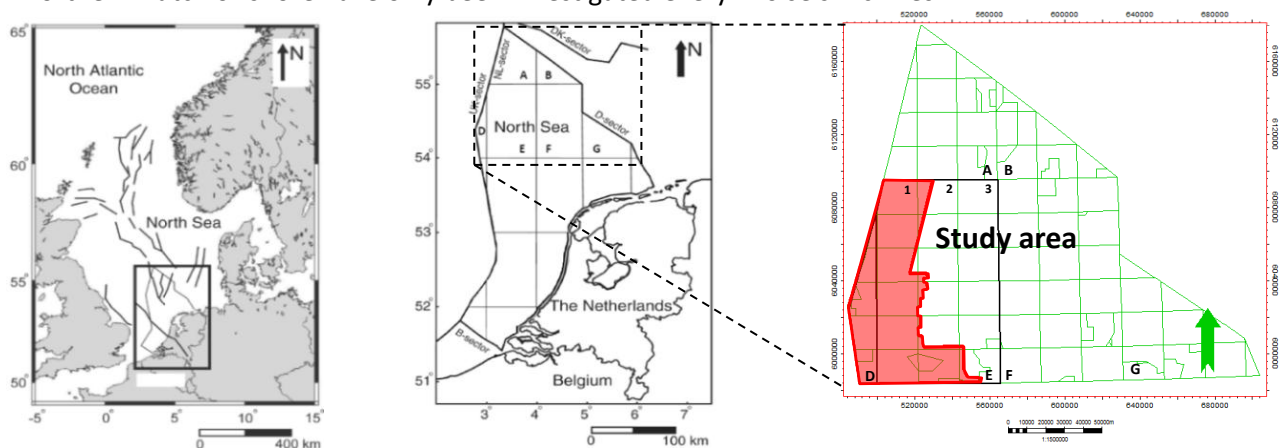


Fig.1) Map showing the northern Dutch Offshore study area. Shaded red indicates the focus area.

1.2.1 Geological setting – Main structural elements

The structural framework of the northern Dutch offshore consists of platforms, highs and basins formed by different tectonic phases. The only high in the study area is the Elbow Spit High (ESH) which represented a high in Permian time and is surrounded by the Elbow Spit platform (ESP) (fig.2). Other platforms in the northern offshore area are the Cleaverbank Platform (CP) in the south and the Schillgrund Platform (SGP) in the east. These platforms are characterized by the absence of Jurassic and partially absent Triassic sediments (fig.2). The most important low in the northern Dutch offshore is the Dutch Central Graben (DCG). This north-south trending graben forms the southern part of the Mesozoic North Sea rift system and is bordered by the shallower Step Graben (SG) in the west and the Terschelling Basin (TB) in the south.

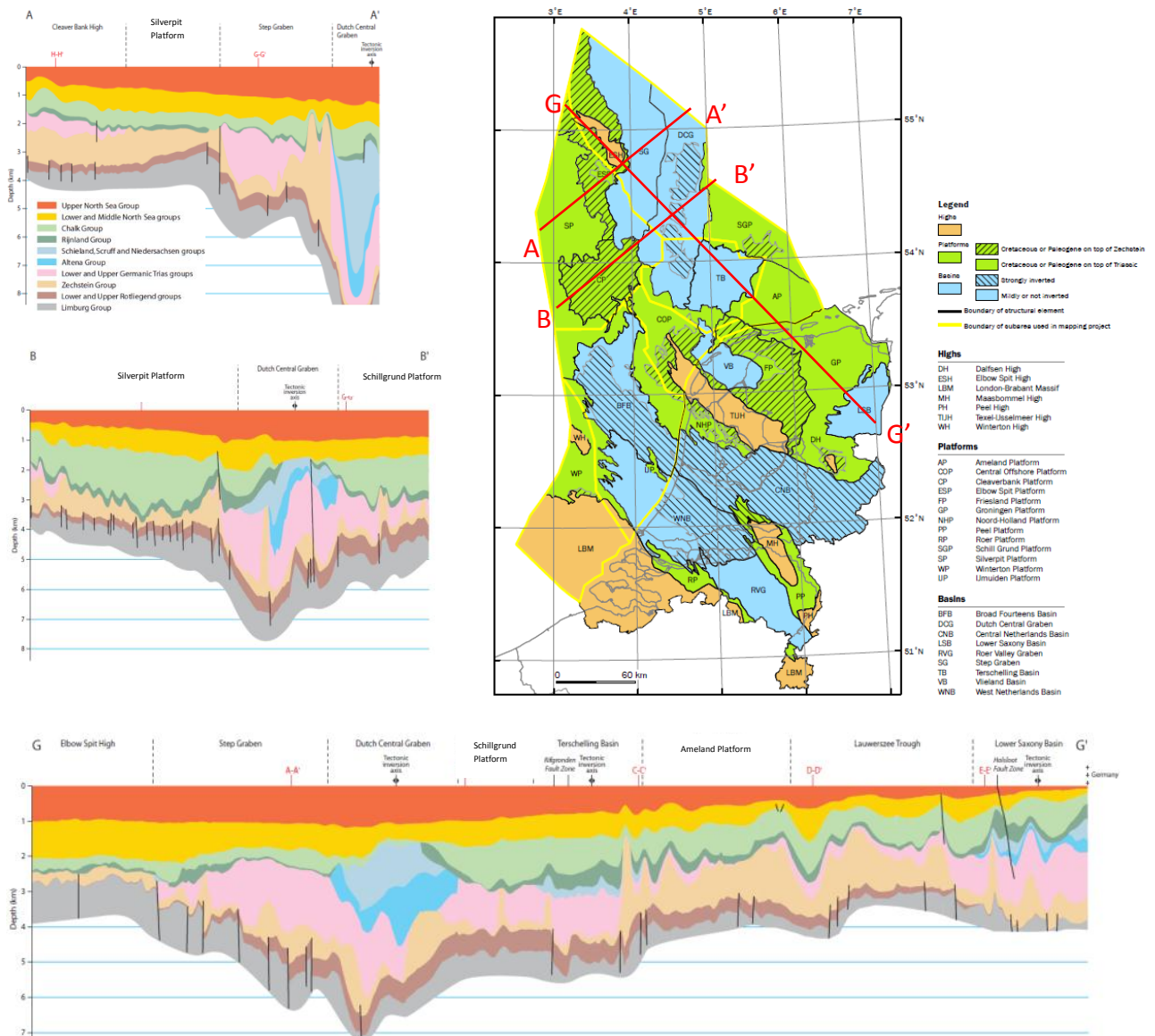


Fig.2) Structural elements map of the Netherlands showing Jurassic-Early Cretaceous basins, highs and platforms (TNO tectonostratigraphic charts, 2011), including three cross sections (Duin et al, 2006)

1.2.2 Geological setting - Lithostratigraphy

The sedimentary succession found in the study area is subdivided into several stratigraphic units which are briefly discussed below (table. 1). The classification is based on the Tectonostratigraphic chart from TNO (2011), which can be found in Appendix D.

System	Series	Group
Neogene	Pliocene	Upper North Sea
	Miocene	
Paleogene	Oligocene	Middle North Sea
	Eocene	Lower North Sea
	Paleocene	
Cretaceous	Upper	Chalk
	Lower	Rijnland
Jurassic	Upper	Scruff-Schieland
	Middle	Altena
	Lower	
Triassic	Upper	Upper Germanic Trias
	Middle	Lower Germanic Trias
	Lower	
Permian	Upper	Zechstein

Table 1) Simplified stratigraphic column based on the Tectonostratigraphic chart from TNO (2011)

Tertiary

The siliciclastic Tertiary deposits of the North Sea Supergroup are subdivided into three different formations; the Upper (NU)-, Middle (NM)- and Lower (NL) North Sea groups (table. 1). The Neogene Upper North Sea group is separated from the Middle North Sea group by the Mid Miocene Unconformity (MMU). This unconformity represents a global low sea-level stand and is known as the “Savian phase” (Kuhlmann, 2004; Wong et al, 2007). The NU represents an alteration of unconsolidated sands and marine clays becoming increasingly clay-rich to the bottom of the section (fig.3). In the Upper North Sea group the sands represent the reservoirs for shallow gas occurrences, whereas the clays represent the seals (Schroot et al, 2003).

Some wells in the research area show a thin package of sand (e.g. well E04-01) and limestone with shell fragments (e.g. well E10-02) on top of the MMU (fig.7). Fig.4 shows the only cored section of the MMU available in the Netherlands, which is not located in the focus area (fig.30). The NU sediments have been formed in a fluvial-, deltaic to restricted marine environment and become thicker towards the northeast in the Dutch Offshore (fig.7) (Wong et al, 2007). These sediments have been deposited by a large scale delta system, known as the “Eridanos delta”, prograding from Scandinavia in the northeast since Late Miocene time (Overeem et al, 2001). Gradually the main sediment supply moved towards the southeast during Early Pliocene time where it converged with the Rhine- Meuse delta system.

The Paleogene Middle- and Lower North Sea groups predominantly consist of deeper marine clays which have been deposited in an outer shelf, low energy environment (fig.5 &7) (Wong et al, 2007).



Fig.3) Core section from B13-03 well. Sediment of Upper North Sea group, consisting of alternating sandstone beds and claystone layers (photo from NLOG website)



Fig.4) Slab cored section from F02-03 well (depth in meters is indicated below core). Sediment of Mid Miocene Unconformity, consisting of a conglomerate of limestone & sandstone clasts in a clay matrix. The green color is related to the glauconitic content

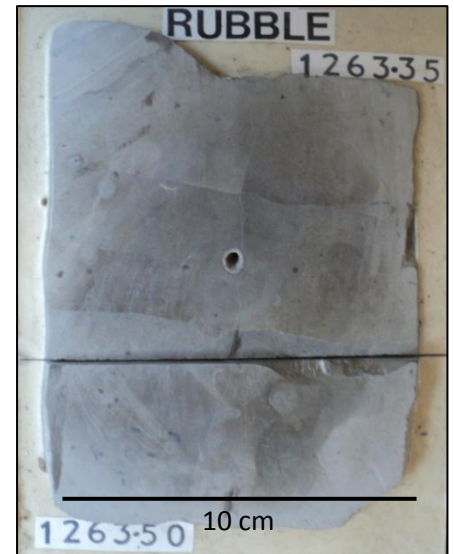


Fig.5) Slab cored section from F02-03 well (depth in meters is indicated below core). Claystone sediments of the Middle North Sea group

Cretaceous

The Cretaceous sediments are subdivided into the Late Cretaceous Chalk group and the Early Cretaceous Rijnland group, which both represent marine conditions (table 1.) (Herngreen & Wong, 2007).

The Chalk group represents a thick sequence of chalk and chalky limestones and is subdivided into the Ekofisk, Ommelanden and Texel formations (fig.6 & 7). Occasionally chert can be observed in the Ekofisk formation, whereas in the lowermost Texel formation marls can be found. The sediments have been deposited in an open marine environment with a low terrigenous influx (Ziegler, 1990).

Sediments of the Rijnland group are subdivided into the Holland- and Vlieland formations. The Holland formation consists of an alteration of marls and claystones and the underlying Vlieland formation predominantly represents claystones (fig.7).



Fig.6) Slab cored section from F02-03 well (depth in meters is indicated below core). Sediment of the Late Cretaceous chalk group is composed of homogeneous bioclastic chalk.

Jurassic

In the northern Dutch offshore Upper-Middle Jurassic (Scruff- and Schieland group) can only be found in the Dutch Central Graben, whereas the Lower Jurassic (Altena group) sediments can be also be found partially in the Step Graben and Terschelling Basin (fig.2).

The Scruff- and Schieland group represent continental as well as restricted marine conditions, and are composed of alternating sand and clays (Wong, 2007). The Altena Group is deposited in open marine conditions and are generally composed of clays. However, in this group also an important source rock can be found, the Posidonia shale formation, which is composed of a bituminous marine shale (Wong, 2007). In the Dutch D- and E quadrants of the study area the Jurassic sediments have not been deposited (fig.7).

Triassic

The Triassic sediments found in the Dutch offshore are subdivided into the Upper- and Lower Germanic Trias groups, however part of this sequence has been eroded in the study area (table. 1). The Upper Germanic Trias group can be found in the Step Graben, Dutch Central Graben as well as on parts of the Silverpit platform (fig. 7). These Middle Triassic platform sediments can be found in the D- quadrants and consist of the Middle Triassic Röt formation (fig.7).

The Lower Germanic Trias group is found in large parts of the area and comprises a succession of the Main Bundsandstein subgroup (e.g. Detfurth and Volpriehausen formation) and the Lower Bundsandstein formations. The Main Bundsandstein subgroup formation consists of an alternation of clays and sands, whereas the Lower Bundsandstein is composed of claystones (Geluk, 2007). These clays have been deposited in a lacustrine environment and the sands represent fluvial deposits. The source for these siliciclastic sediments was the Variscan mountain chain to the south (Geluk, 2007).

Late Permian

Late Permian deposits are known as the Zechstein group, which is mainly composed of marine evaporates such as halite, and carbonate beds (fig.7) (Geluk et al, 2007). This succession has been deposited in the Southern Permian basin, which formed a saline inland sea during a warm and arid climate (fig.8a).

Fig.7) (continues on next page) North-South well log correlation through the focus area (shaded red) as indicated on the maps. From N-S through wells (E02-02, E04-01, D12-05, E10-02, E16-01). Well logs comprise Gamma Ray (GR) and Sonic (DT) log. Legend indicates different lithologies. Colors indicate groups based on age. Dashed lines indicate most important horizons. Question marks indicate unidentified lithologies.

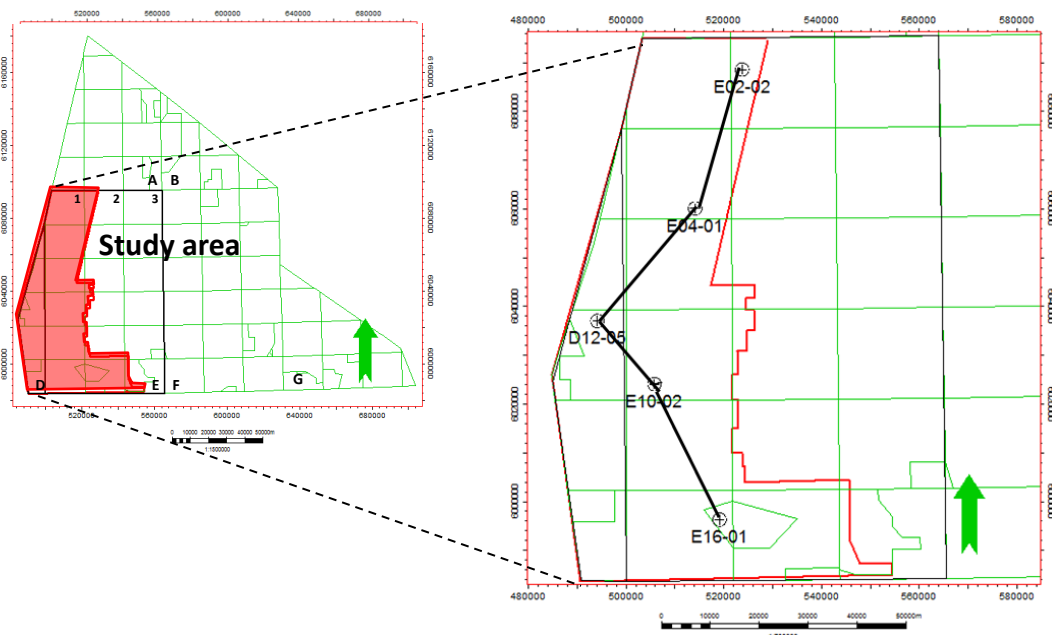
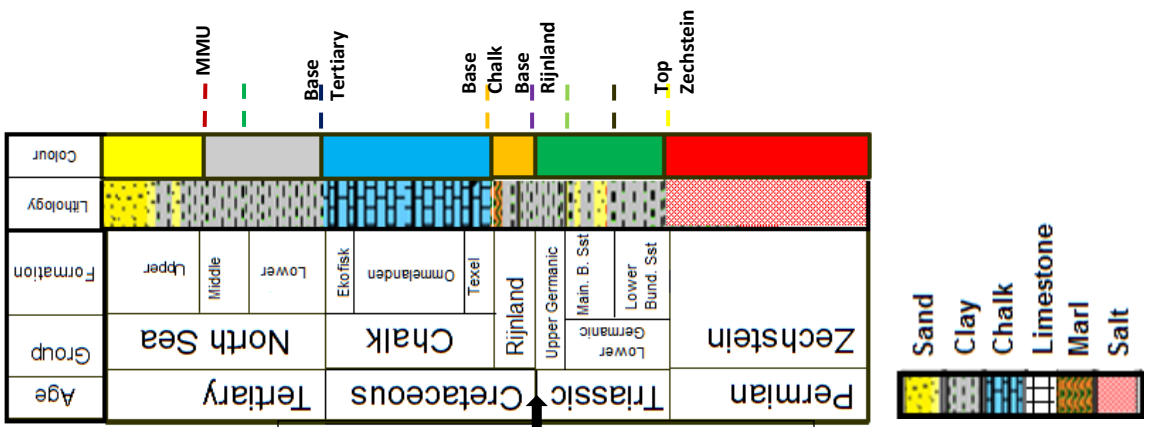
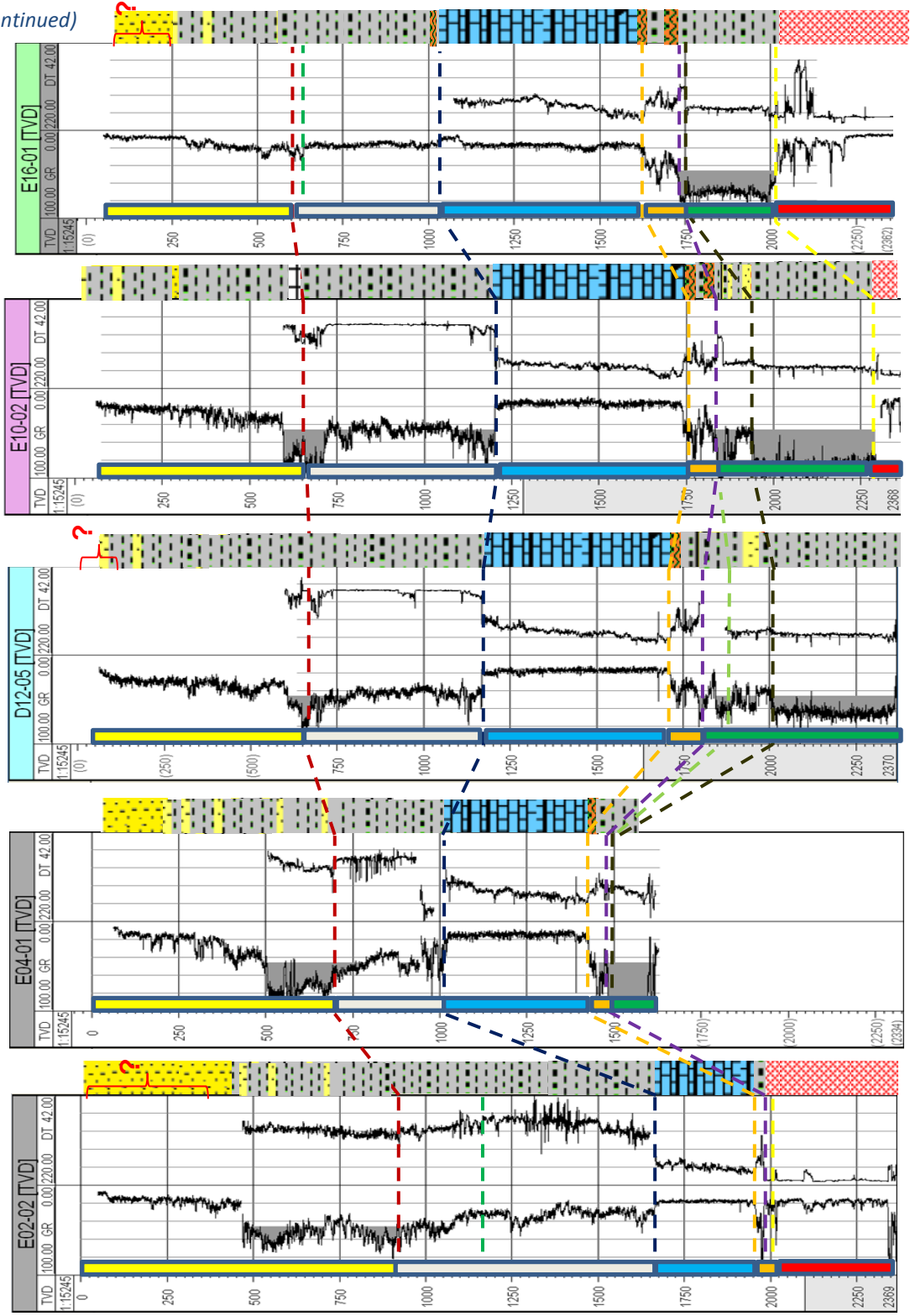
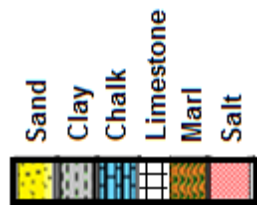


Fig.7 (continued)



Jurassic and Upper Triassic not deposited



1.2.3 Geological History

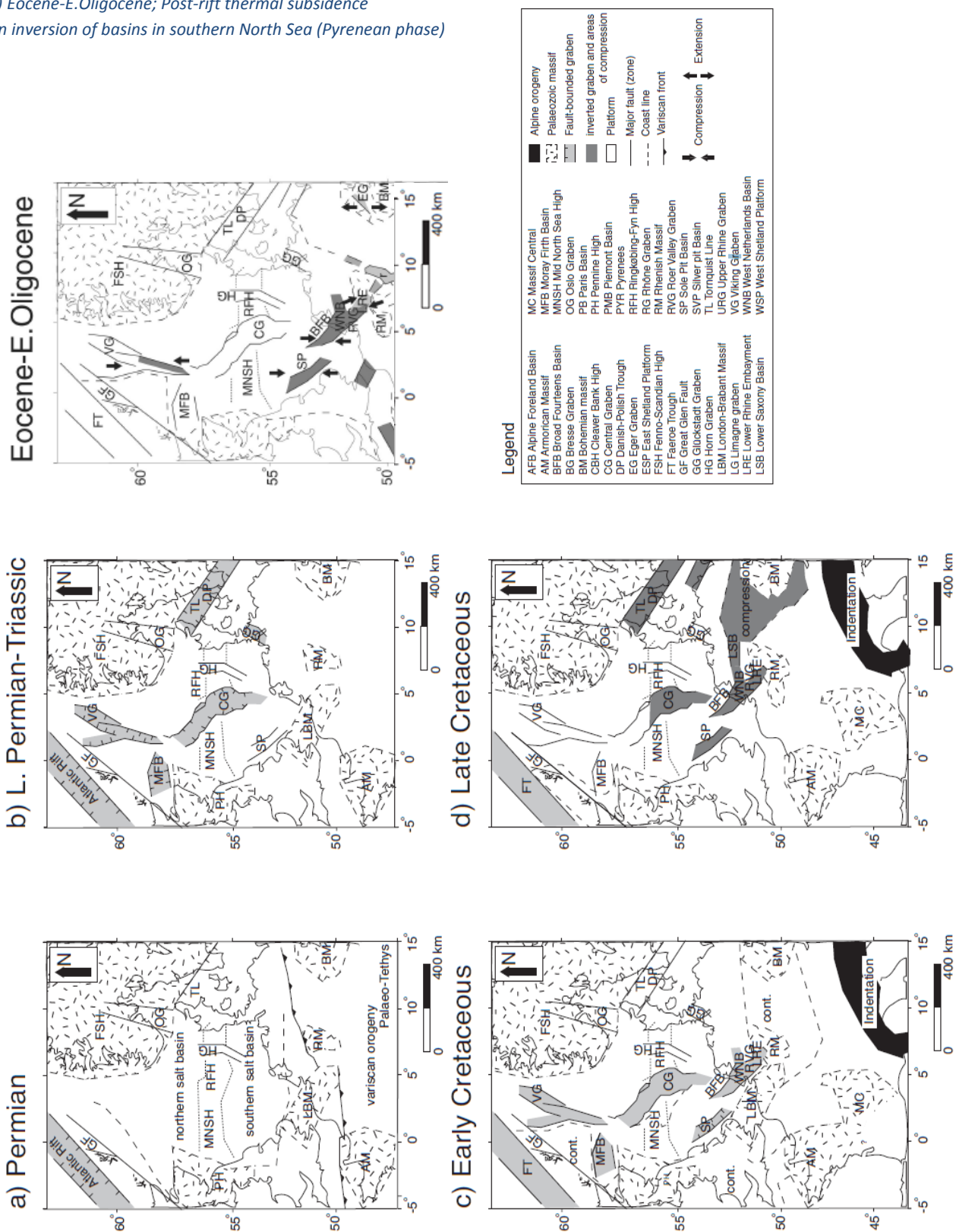
In Paleozoic time, continental collisions occurred between the continents of Laurentia, Baltica and Gondwana which resulted in the formation of the supercontinent Pangea. These orogenic phases are known as the Caledonian and Variscan orogenies which ended during Late Paleozoic time. At the end of the Variscan phase, the Netherlands was part of the intracratonic Southern Permian basin which extended from the United Kingdom in the west, to Poland in the east. This E-W trending basin was bound by the London-Brabant massif and Variscan mountains in the south and the Mid North Sea High (MNSH) and Ringkøbing-Fyn High in the north (fig.8a). The basin developed in response to the Late Carboniferous and Early Permian wrenching/rifting and related volcanism. Late Permian sediments are characterized by the deposition of a thick succession of evaporates and carbonates, known as the Zechstein Group. Continuous loading during Mesozoic and Cenozoic times resulted in the movement and the formation of numerous salt structures in the Dutch subsurface. These structures can be found especially in the northern onshore and offshore regions of the Netherlands. Onset of salt movement started in Triassic time and has influenced sediment deposition ever since (Geluk et al, 2007).

The Mesozoic is characterized by the break-up of Pangea. During Early Triassic time, crustal extension started between Greenland and Norway and propagated towards the Central Atlantic domain (fig.8b) (De Jager, 2007). An eastern branch of crustal extension developed in the North Sea area reaching the southern North Sea during Middle Triassic time. Continued rifting in the western rift branch resulted in continental break up and the opening of the Central Atlantic Ocean between Africa and America in Middle Jurassic. During the Middle Jurassic large parts of the Dutch offshore were uplifted. This was related to the development of the thermal Central North Sea Dome and sedimentation was restricted to the basins, such as the Dutch Central Graben. Rifting in the Netherlands was most intense during the Late Jurassic, which can be seen by the thickness of sediment deposits in the Dutch Central Graben (Ziegler, 1990, Wong et al, 2007). Eventually in Early Cretaceous time, oceanic crust was developed in the North Atlantic Domain and rifting in the North Sea area ceased (fig.8c). The basin experienced post-rift thermal subsidence during Late Cretaceous and Cenozoic time. This cessation in combination with rising sea levels resulted in the deposition of a thick package of chalk sediments in the whole North Sea region (Ziegler, 1990).

The northward movement of Africa and resulting collision with Europe resulted in the Alpine orogeny during Late Cretaceous and Paleogene time. Three major compressional phases can be identified; the Late Cretaceous Subhercynian phase (fig.8d), the Early Paleocene Laramide phase and the Eocene-Oligocene Pyrenean phase (fig.8e). These phases resulted in inversion of the basins present in the southern North Sea, with decreasing intensity to the north. The Subhercynian- and Laramide pulses caused much of the Cretaceous to be eroded in the basins. In Miocene time a phase of global low-sealevel "the Saviian phase" resulted in a sequence boundary known as the Mid-Miocene Unconformity (MMU), which is visible on seismic throughout the North Sea area (Huuse & Clausen, 2001). From the Miocene onwards subsidence continued and a thick succession of deltaic and fluvial sediments were deposited in the basin area. Uplift of the Fennoscandian shield caused a delta system, the Eridanos delta, to prograde from the northeast (Overeem et al, 2001). Gradually the main sediment supply moved towards the southeast during Early Pliocene time where it converged with the Rhine- Meuse delta system.

Fig.8) Schematic tectonic evolution of the North Sea region (from de Lugt, 2007)

- a) Permian; formation of intra-cratonic Permian basin
- b) Late Permian-Triassic; Development of North Sea rift system
- c) Early Cretaceous; Rifting had moved southwards and starts to cease
- d) Late Cretaceous; Post-rift thermal subsidence and inversion of basins in North Sea (Subhercynian phase)
- e) Eocene-E.Oligocene; Post-rift thermal subsidence an inversion of basins in southern North Sea (Pyrenean phase)



2. Background

These sections contain information about two specific types of geological fluid flow expressions; polygonal fault systems and subsurface sediment remobilization. Both these expressions are thoroughly described based on previous research, however there is still much debate on the characteristics and origin of these features.

2.1 Polygonal Fault Systems

Polygonal fault systems (PFS) are usually defined as laterally extensive networks of small extensional faults, which can be found in layer-bound successions (tiers) and show a polygonal geometry in planview (Cartwright, 2011). This section presents an introduction on the global distribution of PFS, the general characteristics and the processes generating them. Despite two decades of research the origin of PFS is still poorly understood.

In the late 1980s, layer-bound extensional faulting was first recognized on 2D seismic data (Henriet et al, 1989). The relationship with sediment compaction and early dewatering had been noticed and PFS were categorized as a new class of soft-sediment deformation process. Not until the widespread use of 3D seismic data, the polygonal planform geometry has been recognized as a key characteristic of these fault systems (Cartwright, 1994). Therefore PFS are often referred to as the subsurface analog for ‘mudcracks’, which are formed by the volumetric contraction as a result of water extraction at earth’s surface (Cartwright and Lonergan, 1996).

2.1.1 Global distribution of PFS

PFS are very common and have been recognized in many sedimentary basins around the world (fig.9). The systems mainly occur at passive continental margins, but can also be found in intra-cratonic and foreland basins (Cartwright and Dewhurst, 1998). Many of the observed networks extend laterally over large distances, such as in the Eromanga basin in Australia ($> 2,000,000 \text{ km}^2$) or in the Paleogene clays throughout the North Sea basin (Cartwright, 2011).

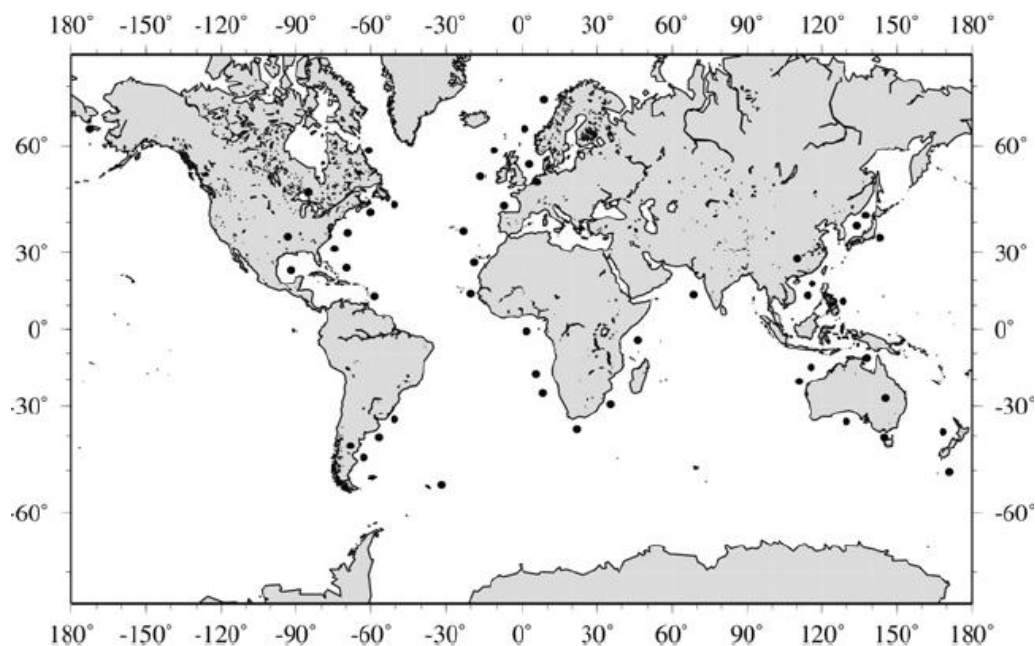


Fig.9) Global distribution of polygonal fault systems (PFS). Black dots represent basins where PFS have been identified using seismic data (from Cartwright, 2011)

2.1.2 Tiers

PFS can typically be found in tiers, which are widely correlatable layer-bound successions, mainly consisting of fine grained sediments in which the extensional faulting is concentrated (fig.10). These fine-grained sediments containing > 70% clay fraction and have been found in lithologies ranging from smectitic rich claystones to almost pure chalk (Cartwright and Dewhurst, 1998; Hansen et al, 2004). Stuevold et al (2003) showed that PFS can also be recognized in tiers where coarser sediments are interbedded into fine-grained sediments.

Tiers can have various thicknesses ranging from 100 meters up to two kilometers (Cartwright et al, 2003). Large faults can sometimes interconnect between tiers through largely undeformed intervals (fig.10). The faulting geometry within tiers depends on the outline and roughly consists of two end-members. Tiers with a constant thickness consist of regular and even numbered faults which are developed in opposite directions (fig.11a). Whereas tiers having a wedge geometry will mainly develop faults dipping towards the thinning region (fig.11b). A combination between these two end members results in the formation of complex tiers, where a large variation in fault size exist (fig.11c).

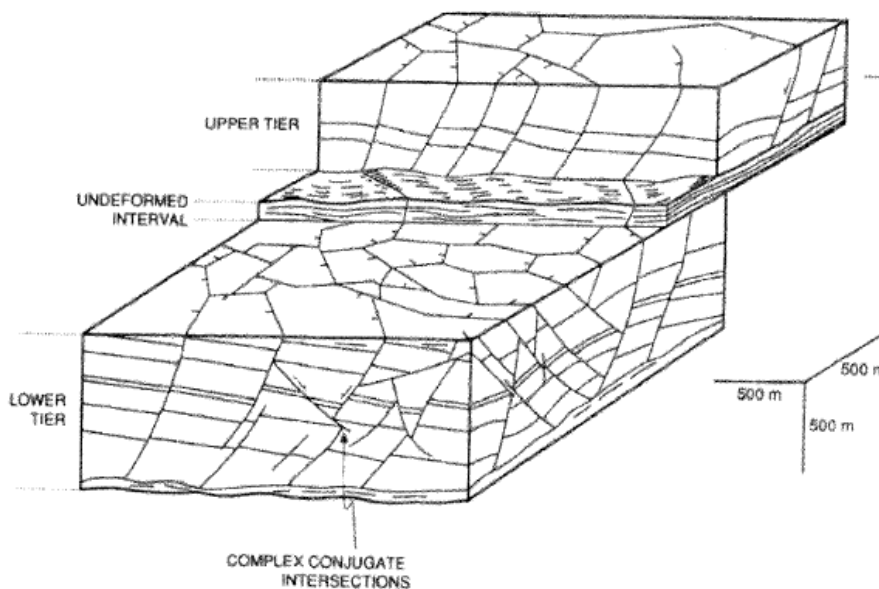


Fig.10) Schematic geometry of PFS showing their organization into tiers (from Cartwright et al, 2003).

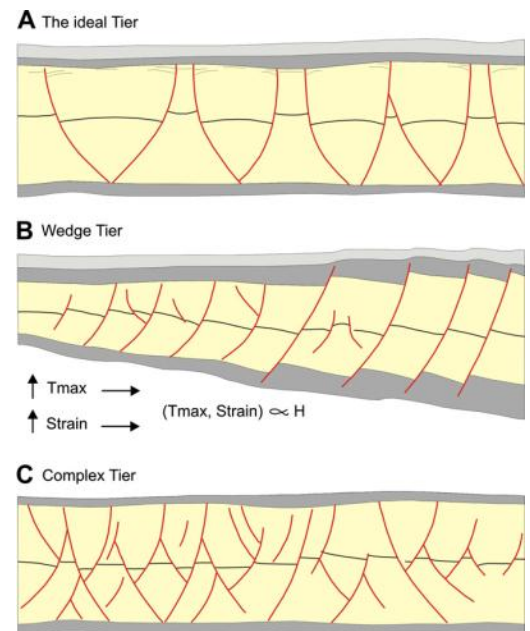


Fig.11) Schematic cross sections through different types of tiers in PFS, a) ideal tier b) wedge tier c) complex tier, see text for further explanation (from Cartwright, 2011)

2.1.3 Fault characteristics

Generally, faults in PFS are planar in tiers up to a couple of hundred meters thickness, but develop a listric character in thicker tiers due to the increased overburden stress. Similarly shallow polygonal faults have dips ranging 50° -80°, whereas deeper buried faults have dips ranging 20° -50°. Both these characteristics indicate a factor of differential compaction of the fault plane and illustrate that the fault geometry depends on the thickness and depth of the tiers involved (Stuevold et al, 2003).

Fault throws in polygonal fault systems increase downward, reaching their maximum displacement in the middle of the interval, and then decrease towards the base of the tier (Gay et al, 2004). Polygonal fault throws generally range between 10-100 meters. Smaller faults probably exist, however these are not observed on seismic data due to seismic resolution limitations.

Similar to measurements on tectonic normal faults, polygonal fault systems also suggest an increase in maximum throw values with larger fault trace lengths (Nicol et al, 2003; Kim & Sanderson, 2005). Fig.12 shows the logarithmic plots of both these fault groups, indicating a linear relationship between the maximum throw values and fault trace lengths. The linear relationship in PFS is more difficult to see and shows a lower slope for the linear trend line. Nicol et al, 2003 attributed this to the high degree of fault linkage, which enables faults to continuously grow in length, and the limited thickness of the tier, which determines the maximum displacement along the fault.

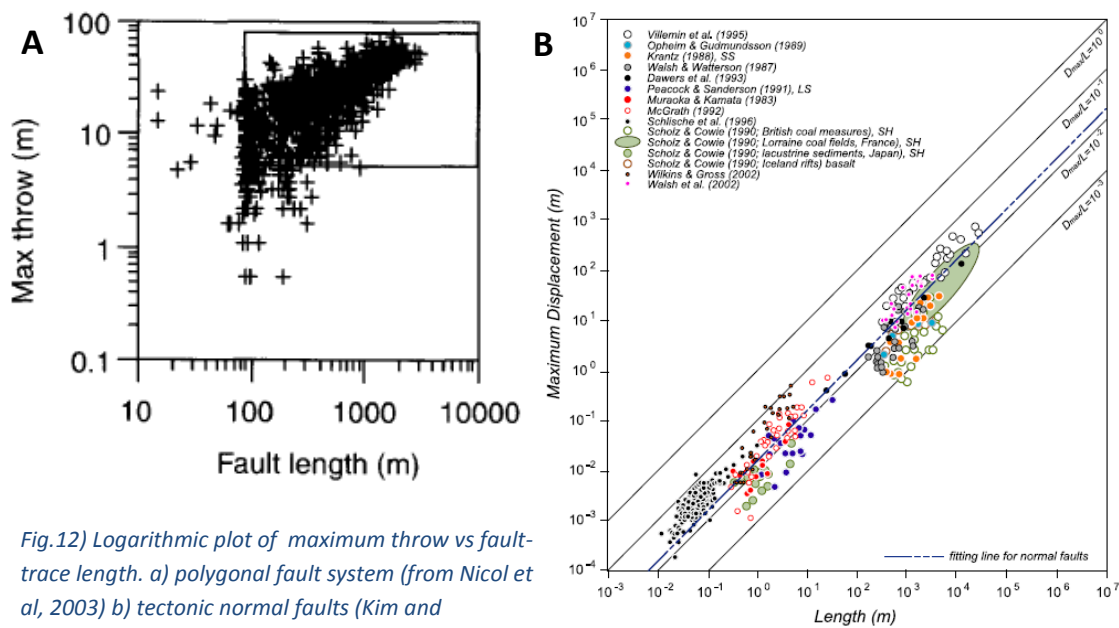


Fig.12) Logarithmic plot of maximum throw vs fault-trace length. a) polygonal fault system (from Nicol et al, 2003) b) tectonic normal faults (Kim and Sanderson, 2005)

Faults can propagate upwards to the seafloor as well, resulting in growth fault sequence development in their hanging-walls (fig.13) (Cartwright and Lonergan, 1996). The Lower Congo Basin, offshore Angola, represents an active faulting environment where a PFS reaches the present day seafloor (Gay et al, 2004). Rectilinear depressions ('furrows') can be seen on the seafloor which are orientated parallel to the basin slope and are located above the faults (fig.14). At the intersection of multiple faults circular depressions (e.g. pockmarks) can be seen on the seafloor, which are characterized by a high drainage potential (fig.14). Furrows as well as pockmarks are indicative of pore fluid escape from the underlying sedimentary sequence. Furthermore pockmarks are often related to fluid and/or gas seepage at the surface, originating from deeper levels (Gay et al, 2004).

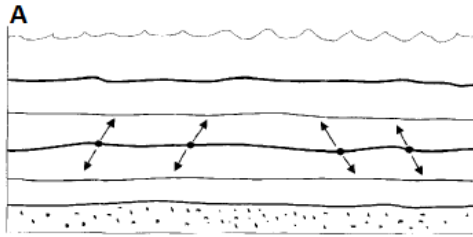


Fig.13 (left) Schematic model for upward propagation of polygonal fault systems. a) initial nucleation of faulting, followed by b) radial propagation until the faults reach the base of the interval and intersect the seabed. Some of the faults do not intersect the seabed and remain 'blind faults' (from Cartwright et al, 2003)

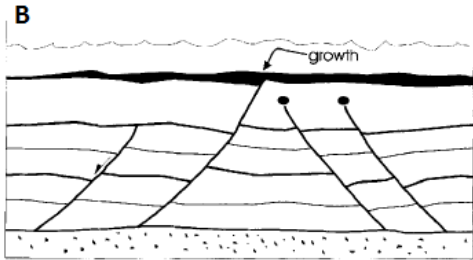
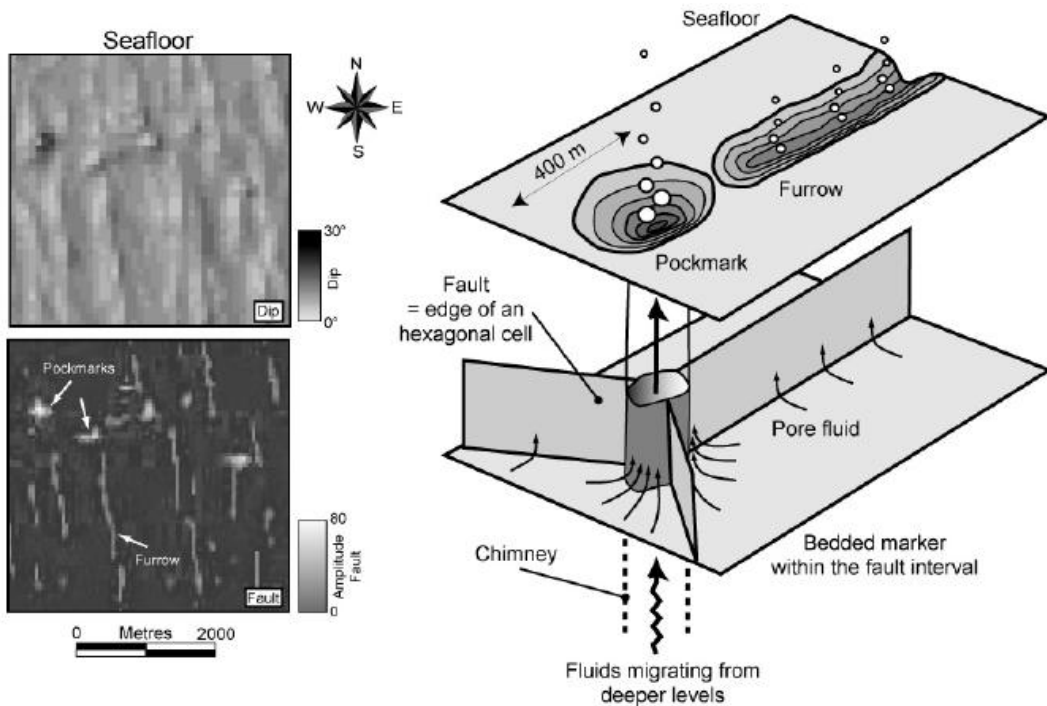


Fig.14 (below) Schematic model showing furrows and pockmarks, and their relationship with fluid pathway in the Lower Congo Basin, offshore Angola (from Gay et al, 2004)



2.1.4 Polygonal planview geometry

PFS are characterized by a polygonal geometry in planview and generally show a large range of strike directions i.e. there is no preferred strike orientation (fig.15). It is this key feature that distinguishes it from other layer-bound fault systems, such as crestal collapse faults (Cartwright, 2011).

Different end-member geometries have been identified for PFS and show varying systems; from highly polygonal (fig.16a), to curved (fig.16B) to rectangular geometries (fig.16c). These variations in polygonal fault geometries are related to the spacing, orientation, intersection and curvature of fault segments. It is important to

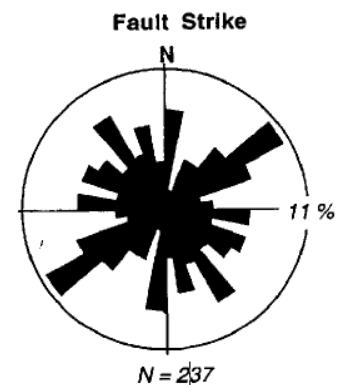


Fig.15) Rose diagram showing an almost equal number of faults in all directions (Central North Sea) (from Lonergan et al, 1998)

remember that there is not a distinct pattern for PFS and that the planform geometry can differ within individual tiers (fig.17) as well as in adjacent tiers (Cartwright et al, 2003). Tiers with a uniform thickness and lithology develop a classical hexagonal pattern in planview, in which faults intersect at $\sim 60^\circ$ and where faults are almost equal in length. These patterns are rare and most PFS are characterized by unequal length distributions and fault intersection angles.

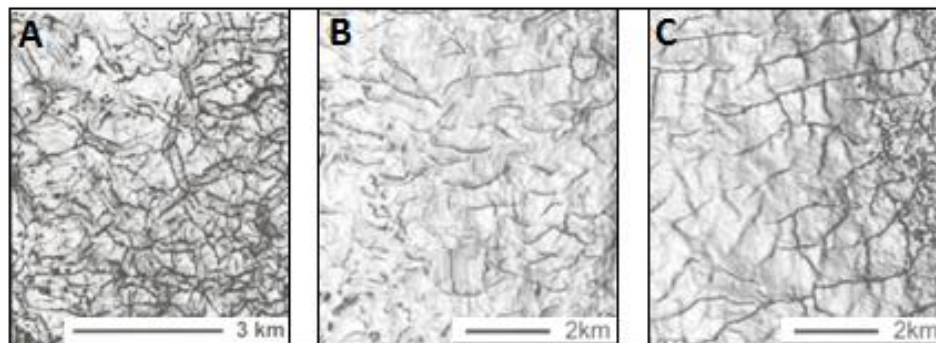


Fig.16) End-member polygonal planform geometries, a) highly polygonal b) curved c) rectangular (from Cartwright et al, 2003)

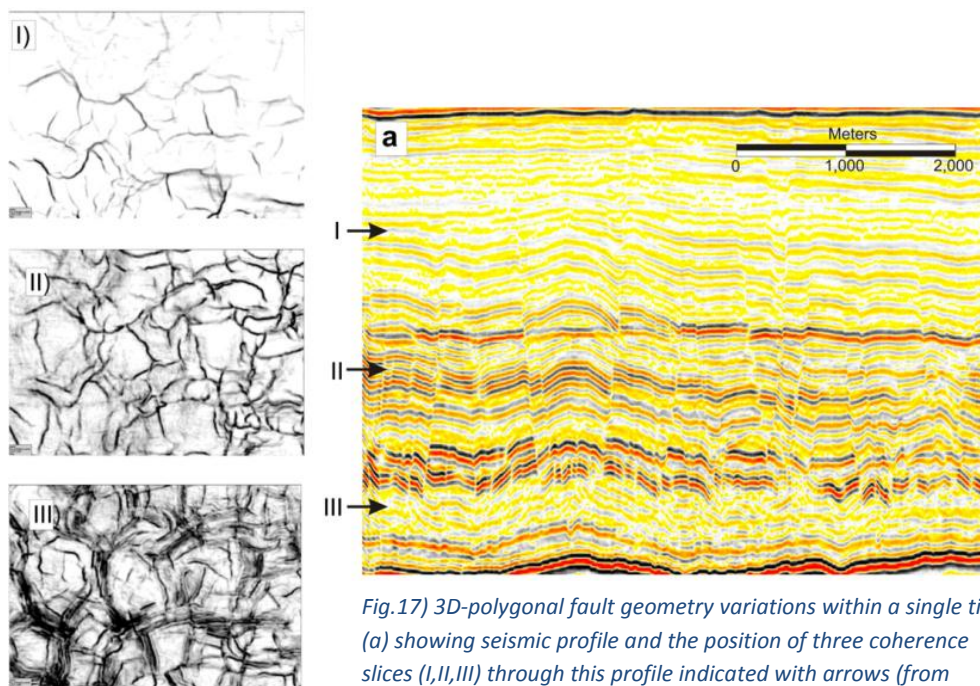


Fig.17) 3D-polygonal fault geometry variations within a single tier, (a) showing seismic profile and the position of three coherence slices (I,II,III) through this profile indicated with arrows (from Cartwright et al, 2011)

The presence of a large range of strike directions in PFS, indicates that there is a horizontal isotropic state of stress where the intermediate and least principal stresses are almost equal ($\sigma_2 = \sigma_3$). The principal vertical stress (σ_1) is formed by the overburden sediments.

Factors influencing the horizontal isotropic stress regime can be related to (regional) topographical changes or the presence of local tectonic stresses, which result in geological structures (Stewart, 2006). For example small changes in the slope gradient at passive continental margins cause a gravitational stress field to be formed, resulting in a preferred fault orientation parallel to the slope contour. Fig 18a shows the effect of levee aggradation adjacent to submarine channels, causing a regional change in topography and related realignment of the faults. Local structures including tectonic faults, salt diapirs, sediment- and igneous intrusions also influence the PFS

geometry and can be superimposed on the original stress regime (Stewart, 2006). The presence of these structures thus changes the horizontal stress regime and the faults do show a preferential strike direction. Fig 18b shows the presence of a salt dome where a radial pattern has formed surrounding it.

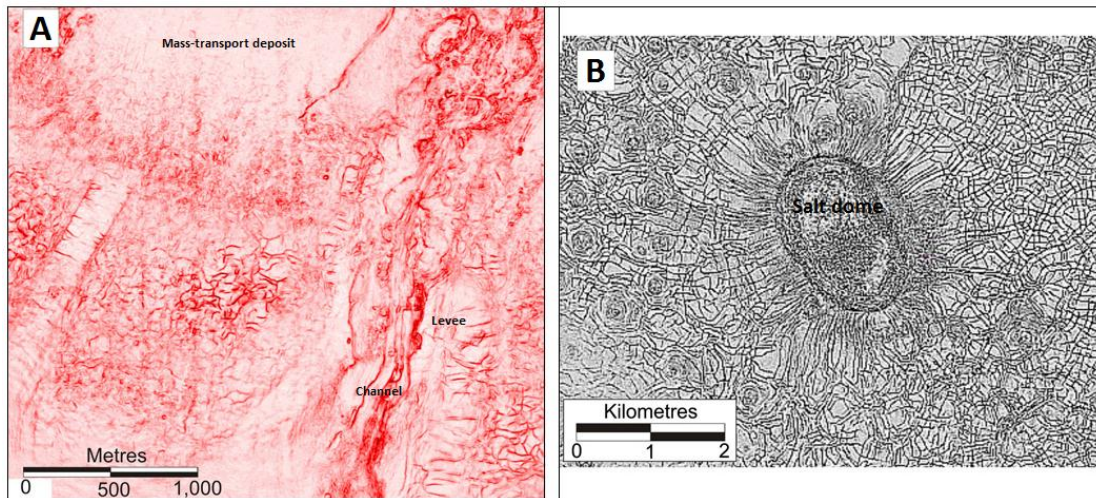


Fig.18) Planform pattern geometry as seen on coherency attribute slices influenced by a) channel-levee system (right) and mass-transport deposit (top) b) salt intrusion (from Stewart, 2006)

The exact influence of lithology on PFS is poorly understood and variation in planform geometries are usually observed in regions where there is an influence of coarse-grained sediment deposits in tiers, such as mass transport deposits or sand bodies (fig.18a). According to Stuevold et al, (2003) PFS can also be found in regions where coarse-grained sediments are interbedded into fine-grained sediments, however there are no known occurrences of PFS found in tiers with dominantly coarse grained sediments.

Laboratory experiments on desiccating muds provide some analog information on the planform geometry observed in PFS. Experiments from Grosiman and Kaplan (1994) show that there is a relation between the scale of the fault pattern and the thickness of the desiccating mud layers. Thin rapidly desiccating muds form closely spaced short fractures as a result of the initiation of many faults at the same time, whereas slower desiccating thick muds tend to form wider spaced rectangular faults. Boundary effects such as friction with the layer beneath the mud, and lithological heterogeneities also affect the fault pattern developed in these muds.

2.1.5 Genesis of PFS

Polygonal faults originate at shallow depths beneath the surface in consolidating sediments and are related to continuous dewatering (Cartwright, 1994). This dewatering causes a re-orientation of the grains and associated volumetric contraction of the layer (fig.19). Eventually, this results in the development of polygonal faults. However, the exact mechanism why these faults originate is still matter of debate.

Several difficulties associated with the origin of PFS continue to be poorly understood, for example the shallow compaction of fine-grained sediments relates PFS to soil-mechanics rather than rock-mechanics. However the observed 3D-consolidation during PFS formation contradicts with the classical 1D-consolidation of soils. Furthermore the observation of brittle-deformation at shallow depths remains difficult to explain. To better understand the origin and influence of PFS more research and technological improvements are required.

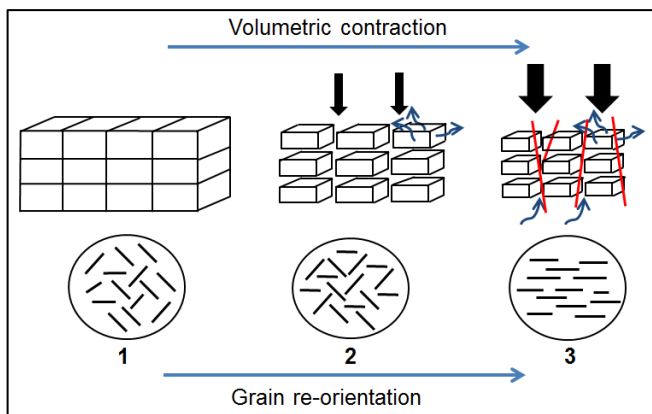


Fig.19) Schematic image of continuous dewatering during burial. 1) deposition of sediment with high porosity and water content. 2) grain reorientation, associated water expulsion and volumetric contraction during burial, creating voids. 3) Voids act as conduits for fluids from deeper levels

Several models have been proposed for the genesis of PFS and these will be explained below. The models have not been addressed any further in this research to explain the origin of the Paleogene polygonal fault system observed in the northern Dutch offshore.

Density inversion

Henriet et al (1991) propose a density inversion model that explains the genesis of PFS. Compaction of fine-grained sediments at shallow depths is preferred close to coarser-grained sediments, causing seals to be formed (fig.20 a&b). Less compacted sediments can be found below more compacted sealing sediments, which can lead to density inversion. Additional overburden causes folding of inverted- sediments, the build-up of pore-fluid overpressures and gravitational instability (fig.20 c). Eventually, faulting of the folded regions leads to the seal-collapse, which in turn releases the overpressures and causes compaction of the underlying sediments (fig.20d).

Watterson et al, (2000) stated a refined density-inversion model, where faulting occurs above the folded regions instead of inside the folded region itself.

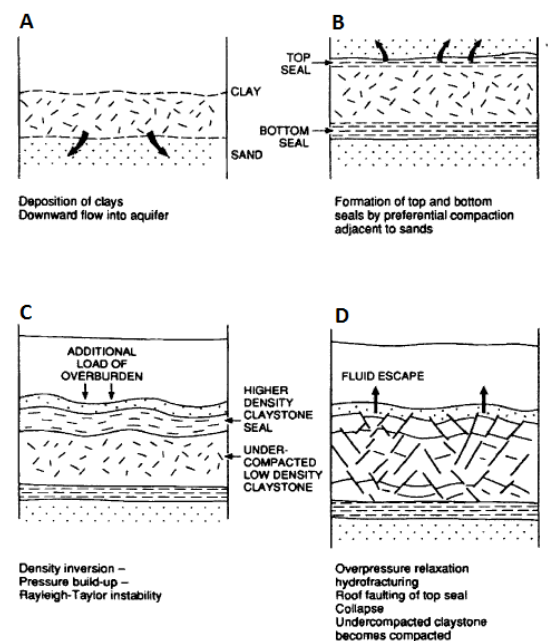


Fig.20) Schematic genesis model for PFS via density inversion after Henriet et al, 1991. a) deposition of sediments b) seal formation c) density inversion folding d) polygonal faulting and fluid escape (from Cartwright et al, 2003)

Syneresis

A model was introduced by Cartwright and Dewhurst (1998) in which syneresis causes the fine-grained sediment sequences to be fractured. Syneresis is the spontaneous expulsion of a liquid from a gel (contraction) without evaporation of the liquid. A similar process occurs when yoghurt passes the expiration date and whey forms at the surface. The fine-grained sediments can act as this gel, due to the inter-particle forces developed between marine clays in sea-water (Dewhurst et al, 1999). Differences in the balance of these forces depend on the size, structure and composition of the sediment particles. Changes in the electrochemical environment cause parts to synerize, where the particles in the gel move together due to a net increase in inter-particle attractive forces, resulting in fault nucleation (fig. 21 a&b). Permeability along faults is increased, causing more pore-fluid escape along the fault (fig.21 c).

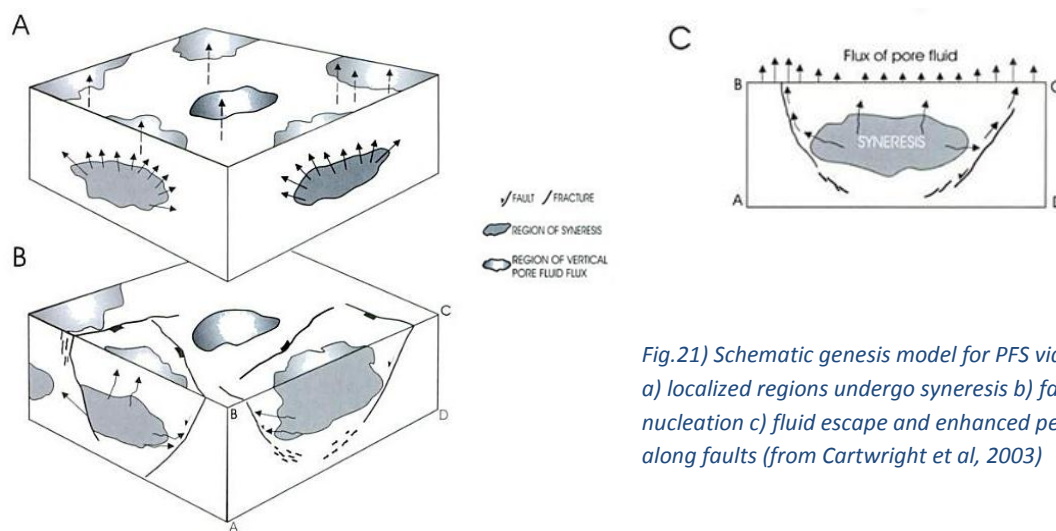


Fig.21) Schematic genesis model for PFS via syneresis a) localized regions undergo syneresis b) fault nucleation c) fluid escape and enhanced permeability along faults (from Cartwright et al, 2003)

Low coefficients of friction on fault planes

The low-friction coefficient model from Gouly (2001) is based on the assumption that clay-sized sediments are so weak, that fracturing will occur due to gravitational loading and no additional tectonic stresses or overpressures are needed. Faults continue to grow due to increased loading of sediments, but only when the residual friction-coefficient on fault planes remain sufficiently low. However, this model does not explain how the faults originate at the grain scale, as sediments tend to consolidate simply by grain scale micro-slippage rather than faulting (Cartwright et al 2003).

Gouly et al (2008) proposed a revised model in which the initiation of faulting occurs at sites of inhomogeneities in the sediments due to differential compaction. These inhomogeneities, such as lateral lithological variations, bioturbation features or shell remains, could be sites where stresses are build-up which in turn lead to the nucleation of small faults.

Shallow diagenetic processes

The most recent model that explains PFS is proposed by Shin et al (2008). According to this model, failure occurs due to early diagenetic (chemical) changes in compacting fine-grained sediments. Diagenetic reactions start during burial of sediments and can continue until metamorphism begins. Shallow diagenetic reactions can either lead to physical grain removal, for example by dissolution, or chemical changes on mineral surfaces which influence the mineral-mineral interactions and mineral-pore fluid interactions (Cartwright, 2011).

Dissolution causes porosity reduction and a structural rearrangement of the grains, resulting in the volumetric contraction of the sediments. This contraction can reach the condition for shear failure in frictional granular materials, which is given by a critical value for the ratio of horizontal to vertical effective stresses. Faults may then localize at grain-level, and a “chain-reaction” can cause the unconsolidated sediments to fracture up to meter scale. When the porosity reduction is sufficiently large, these physical property changes can be seen on seismic reflection data, since these depend on acoustic impedance differences. For example the diagenetic reactions of silica from opal-A (dissolution) to opal-C/T (precipitation) cause a marked seismic reflection (Davies et al,2009). Praeger (2009) investigated cores of diagenetically altered volcanic ash deposits in the Nankai Trough in Japan where the alteration process caused porosity reduction which could be related to PFS formation.

Several other reactions could also be candidates for diagenetically induced fracturing, for example; dissolution of detrital calcite and aragonite, anaerobic methane oxidation, remineralisation of organic matter and reactions related to microbial activity. Many of these reactions influence the physical properties on a grain scale and can be possibly related to macro-scale processes. A combination of these diagenetic reactions might possibly explain the PFS found in different sedimentary settings and their occurrence over enormous lateral distances.

2.2 Subsurface Sediment Remobilization

The process of subsurface sediment remobilization is related to significant fluid movements in the subsurface and has been studied in many sedimentary basins around the world. Since the beginning of the 20th century onshore fluid flow expressions, such as mud volcanoes have been recognized (Kopf et al, 2002). Whereas these features have only been found offshore and in the subsurface during the last few decades, especially with the widespread availability of 3D-seismic data (Huuse et al, 2010).

These post-depositional structures are formed due to the forceful injection of sediments (<1 km depth) into usually overlying sealing lithologies, in which the grains are being carried by the ascending fluid flow. This remobilization of unconsolidated sediments might be related to undercompaction, caused by the rapid burial and low permeability inhibiting efficient pore water escape (van Rensbergen et al, 2003).

Traditionally, subsurface sediment remobilization has been grouped into two different lithological systems; “sand injection systems” and “mud volcano systems”, where the sand injection systems typically represent intrusive features and the latter represent extrusive features. This classification was based on the assumption that these structures formed differently and independently. However, this view has recently been challenged and these systems show similar characteristics and may have the same processes involved in their generation (Huuse et al, 2010).

2.2.1 Sand injection systems

Sand injection systems can be subdivided into three structural elements; a parent unit, which supplies the fluid and sand that becomes remobilized, an intrusive belt, where dikes and sills are formed, and an area of sand volcanoes and extrusions, if the surface is reached (Huuse et al, 2010). Over 90% of the sand injection systems identified at present represent intrusive features (Andresen et al, 2009). The injections can have various geometries and range in size from cm- to kilometer scale (fig.22). Some of the injections even inject downward (Andresen et al, 2012). The injection systems have been identified on outcrop data, in wells and on seismic data (fig.23&24).

Injections typically involve fine-to medium grained quartz sand, but recent study showed that these can also involve conglomerates and breccias (Szarawarska et al,2010). Porosities and permeabilities are usually good and range up to 40% and 1-10 Darcy respectively. These characteristics make sandstone intrusions excellent migration pathways for ascending fluid and/or hydrocarbons even up to millions of years after their formation. However, occasionally laminations can be observed in the injections, which are formed by post-emplacment processes such as cementation and deformation bands influencing fluid migration and possibly represent barriers to flow (Jonk, 2010).

Large scale sand injections can form saucer shaped (“winglike”) (Polteau et al, 2008) or conical (“V-shaped”) (Shoulders et al, 2007) intrusions which can be identified on seismic data (fig.24). These injections are generally characterized by high amplitude reflections compared to the surrounding reflectors. These reflections can be seen as dikes, which crosscut the bedding, and as sills, which form parallel to the bedding (fig.24).

These sand injections are typically found at 15-45° relative to the parent body and are between 100 to 300+ meters high (Huuse et al, 2012). Crestal complex intrusions are more difficult to identify on seismic data since these resemble a complex set of thin sills and dikes. Fig. 23C shows an example of the Panoche Giant Injection Complex in California which represents the only large scale crestal complex outcrop in the world.

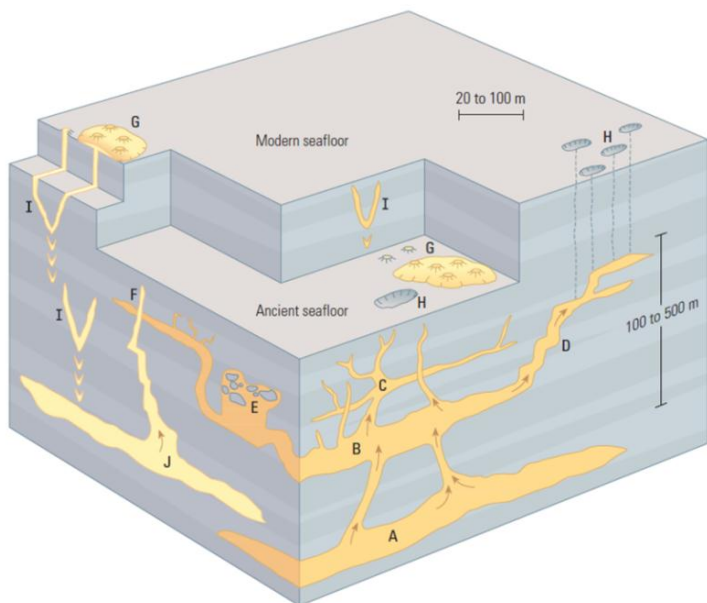


Fig.22) Common sand injection features A; Depositional parent sand body. B; Thick sill C; Crestal Intrusion complex. D; set of sills which link with dikes in a step fashion (“winglike”). E; large irregular intrusive body, which contains clasts of host rock. F; sill originating from parent body A which is crosscut by a dike from parent body J. G; Sand volcanoes and extrusions. H; gas seeps. I; Conical sand injections (“V-shaped”) (from Braccini et al, 2008)

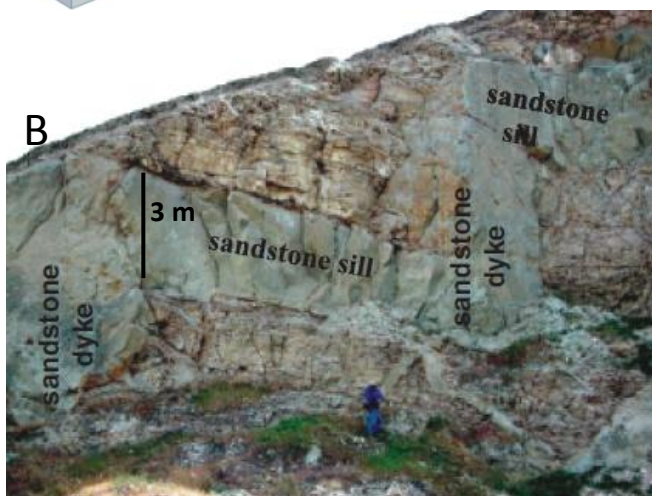


Fig.23) Examples of sandstone intrusions A) Sandstone dike in well from Tullich field (~10 cm thick) (from Hurst et al, 2007) B) Dikes and sills from outcrops in California, USA (~3 m thick) (from Jonk et al, 2010) C) Giant Panoche Intrusion Complex, California (from Huuse et al, 2012)

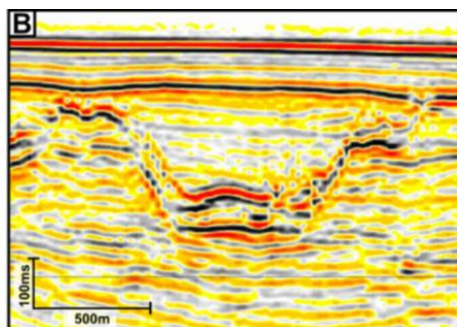
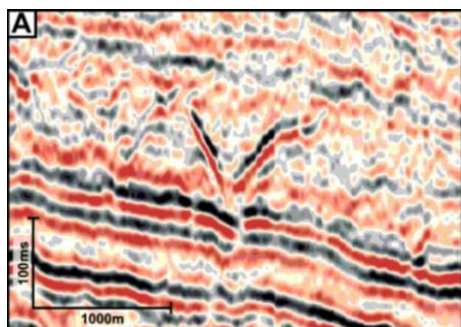
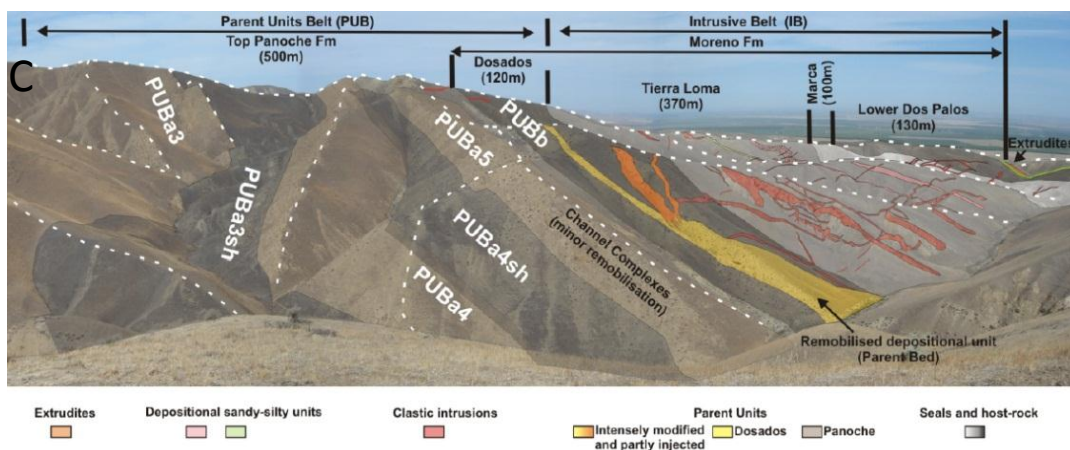


Fig.24) Seismic scale sandstone intrusions A; Conical B; Saucer-shaped (from Cartwright, 2010)

2.2.2 Mud volcano systems

Mud volcano systems can be subdivided into three elements; the extrusive mud volcano, the intrusive domain and the parent source layer (fig.25) (Stewart and Davies, 2006). Mud volcano systems can be deeply rooted, up to 3 km, but mobilization can also take place at shallow depths (< 1000 m). Mud volcano systems can be found in two regions: those found in petroleum regions, related to hydrocarbon generation and those in magmatic regions, related to hydrothermal fluids (fig. 26 B&C) (Mazzini, 2009).

The mud volcano systems have been identified in outcrops, in wells and on seismic data (fig.26 & 27). Mud volcano systems are usually found as extrusive features (90%) because the intrusive parts have a low preservation potential in outcrops (Huuse et al, 2010). Furthermore, on seismic data the intrusive domain is often difficult to image due to overburden gas (Stewart and Davies, 2006). The extrusive mud volcano is described as a positive relief structure seen on the surface from which mud and fluids erupt or flow. The mud is often composed of a mud-fluid mixture, which can contain sand and consolidated mudstone fragments (Roberts et al, 2010). Sizes of mud volcanoes range from large cones up to 3-4 km in diameter and 400 meters high to small meter-sized cones of liquefied mud and gas (fig. 26 B,C,D) (Loseth et al, 2009).

Mud volcanoes show a periodical cycle of eruptions which can range from days to thousands of years and evidence for repeated mud flows can often be seen (Roberts et al, 2010). This periodicity appears to be controlled by the local pressure regime within the sedimentary sequence (DeVillie, 2006). On seismic data stacked mud volcanoes have been identified which represent long-lived structures lasting up to several millions of years. However, studies of actively erupting mud volcanoes are rare due to their unpredictable behavior and usually form in inaccessible places, such as (deep) water. The Lusi mud volcano eruption of 2006 in Indonesia provided an unique opportunity in this respect and resulted in valuable information on the evolution of mud volcano systems (fig.26C) (Roberts et al, 2010).

The intrusive domain is the least understood part of mud volcano systems but also the most important since this penetrates the overlying seals and make them effective seal bypass systems (Cartwright et al, 2007). Until recently it was thought that this part was represented by a km-scale mud-diapir complex. This view has been challenged and it is questioned whether these diapirs can physically exist in the subsurface (DeVillie, 2006; Roberts et al, 2010) (fig.28). Furthermore, improved seismic imaging revealed that this domain was previously interpreted wrongly due to difficulties associated with imaging vertical structures. Research shows that the intrusive domain is represented by a mud dike, sill and feeder-pipe complex (Stewart and Davies, 2006, Roberts et al, 2010). The mud is transported through linked dikes and sills which range in thickness from cm to meters (fig. 26a).

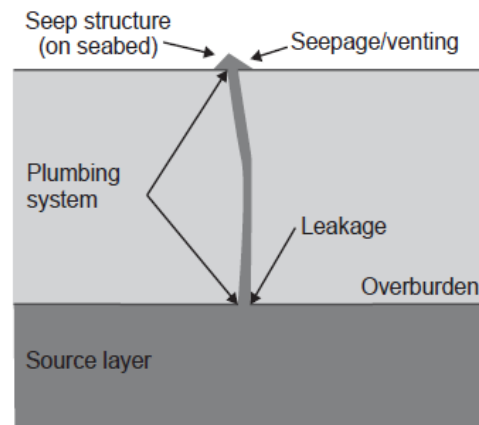


Fig. 25) Schematic figure showing the three structural elements of mud volcano systems. Sizes can range from meters to hundreds of meters (Talukder, 2012)

The intrusive domain can be recognized on seismic data as vertically stacked anomalies of chaotic reflections, similar to gas chimneys (Loseth et al, 2009) (fig.27). The mud volcano is recognized as a “mounded” relief overlying the chaotic domain and influences nearby seismic reflections. These influences include onlap onto the volcano, if sediment reaches the paleo surface and “draping” of sediments overlying the mound, caused by differential compaction between the volcano and succeeding sediments (Andresen et al, 2010).

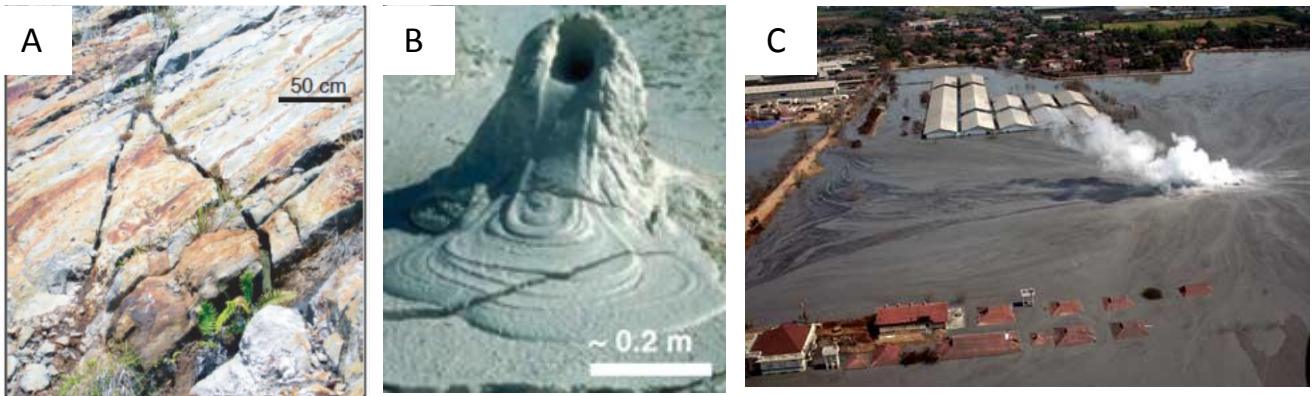


Fig.26) Examples of mud volcano systems a) Mudstone dikes in sandstone, Brunei (Morley et al, 2003) b) Mud volcano from Yellowstone National Park, USA (USGS website) c) Lusi mud volcano, Indonesia d) Tuorogai mud volcano Azerbaijan (Mazzini et al, 2009)

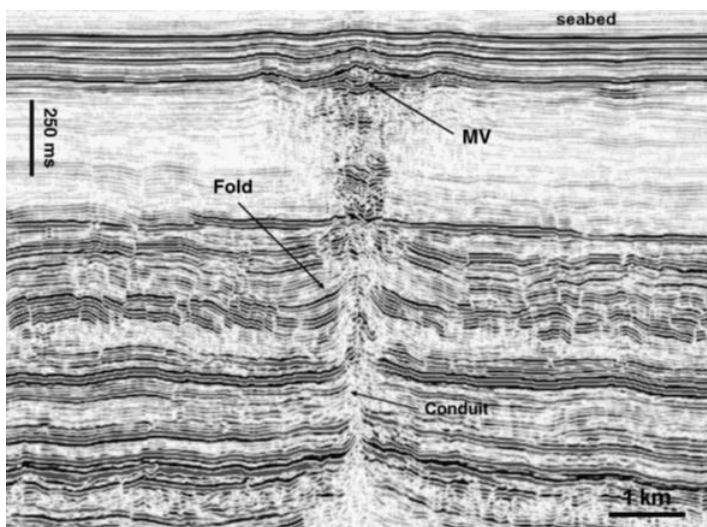


Fig.27) Seismic expression of a buried mud volcano (MV) and underlying cylindrical conduit (Hansen et al, 2005)

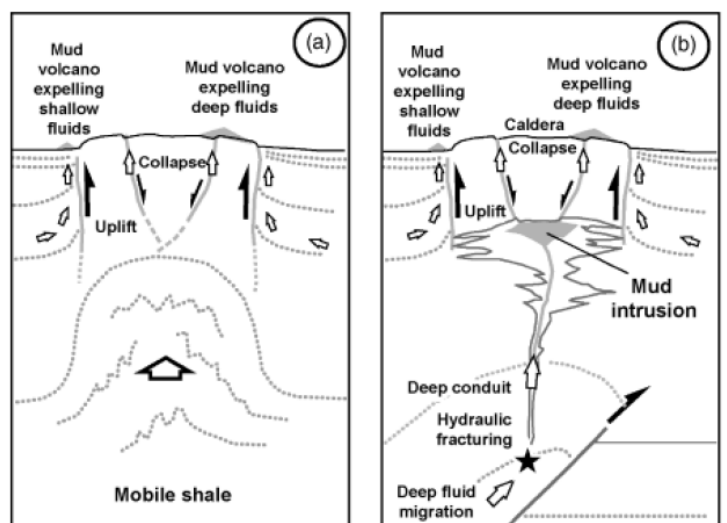


Fig.28) Two hypotheses about the origin and underlying structures associated with mud volcanoes a) mud-diapir complex b) mud dike, sill and feeder-pipe complex (DeVilleville, 2006)

2.2.3 Generation mechanisms

Both mud- and sand remobilization are initiated by pore-fluid overpressures and generally activated by an external trigger, to start hydraulic fracturing and associated injection (Huuse et al, 2010). However, shallow mud remobilization might also be driven by biogenic (internal) hydrocarbon production in a thick overpressured mudstone, attributed by the internal fluid expulsion of these compacting sediments (Loseth et al, 2003).

Pore fluid overpressure generation can be related to different processes; disequilibrium compaction due to rapid burial, causing part of the fluids to remain entrapped in the pores, lateral transfer of pressure, due to tectonic tilting and differential loading, hydrocarbon generation, which can have a biogenic as well as thermogenic origin, silica and carbonate diagenesis (for example; opal-A to opal-CT reaction) and cementation, causing pore pressure reduction (Osborne and Swarbrick, 1997; van Rensbergen et al, 2003). These overpressure mechanisms do not build up pressures quickly enough for hydraulic fracturing to occur at these shallow depths (< 1km). Therefore it is thought that they rather act as a pre-conditioning mechanisms for sediment remobilization and the need for an external triggering mechanism is suggested to start the injection event. Furthermore to produce large scale remobilization structures an external fluid source is needed.

The trigger mechanisms include seismic- (e.g. earthquake) and impact shaking (e.g. meteorite), instantaneous loading events (e.g. submarine landslides) or a sudden release of fluids along active fault planes (Cartwright, 2010). These mechanisms cause a sudden increase of overpressures and cause the development of a fracture network. If pre-existing weaknesses already exist, such as polygonal faults, these will be exploited by the ascending fluids (Lonergan et al, 1998)

When the fluid flow velocity is high enough, sediments can become entrained in the ascending fluid and get injected along the fractures. This fluidization of sediments depends primarily on velocity, relative density and particle size, but also on fluid viscosity (Jonk et al, 2010). Expulsion of sediment at the surface is often related to gas being expelled from the fluid in the shallow subsurface, reducing the relative density of the material and favors sediment remobilization (deVille et al, 2010). The incorporation of different grain sizes and wall rock causes a greater fluid viscosity and density of the mixture. This enables larger clasts to become entrained in the fluid flow, such as pebbles and cobbles.

3. Data and Methods

In this research multiple datasets have been used including 3D seismic data, well logs and a cored well section. These datasets have been combined and analyzed in Schlumberger's Petrel software. First, a short description of the seismic data will be given, followed by the available well data. Finally the workflow related to the Petrel software and the analysis on the mounded structures and polygonal faults is explained.

Data

3.1 Seismic data

The seismic data available for this study comprises public 3D seismic surveys from the northern Dutch offshore quadrants A- to G (fig.29). These seismic surveys have been merged together in a giant survey, known as "Terracube" (purple outlines). Furthermore, part of the 2012 3D multi-client "DEF survey" shot by Fugro in the D, E and F quadrants has been used in this research (blue outline). The line spacing for the merged Terracube survey is 25 meters, whereas in the 2012 "DEF survey" inline spacing is 25 meters and crossline spacing is 12,5 meters. The 3D seismic surveys combined cover a large part of the northern Dutch offshore. This study focuses on the under-explored offshore D- and western E quadrants as indicated in figure 29 (red outline).

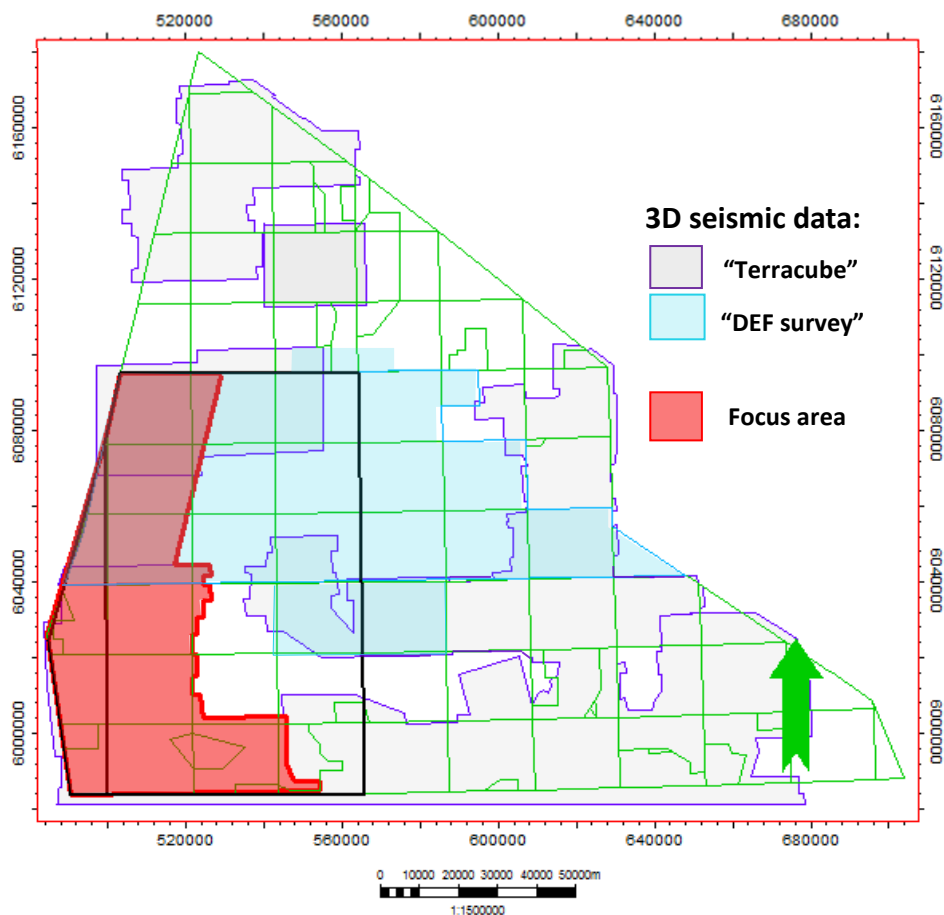


Fig.29) Map showing 3D seismic data outlines in the northern Dutch offshore

3.2 Well data

Well data used in this study have been imported from the Netherlands oil and gas portal website (<http://nlog.nl>) (fig.30). This site comprises all publically available data as is being managed by TNO, the Geological Survey of the Netherlands. The data gathered from the site includes location, deviation, well logs and interpreted well-tops from all the wells available in the Netherlands. Well information is available 5 years after drilling, therefore the most recent wells have not been used in this research. Well log data includes a gamma ray, sonic, density and resistivity measurements. The available wells in the study area have been analyzed, with the focus on Cenozoic sediments. All wells were drilled with an objective below the Paleogene sediments and in many wells detailed information on these sediments is sparse.

Only one cored section of the Middle- and Lower North Sea group is available at the TNO core house in Zeist, from the F02-03 well. This core has been analyzed and documented (fig.4 &5).

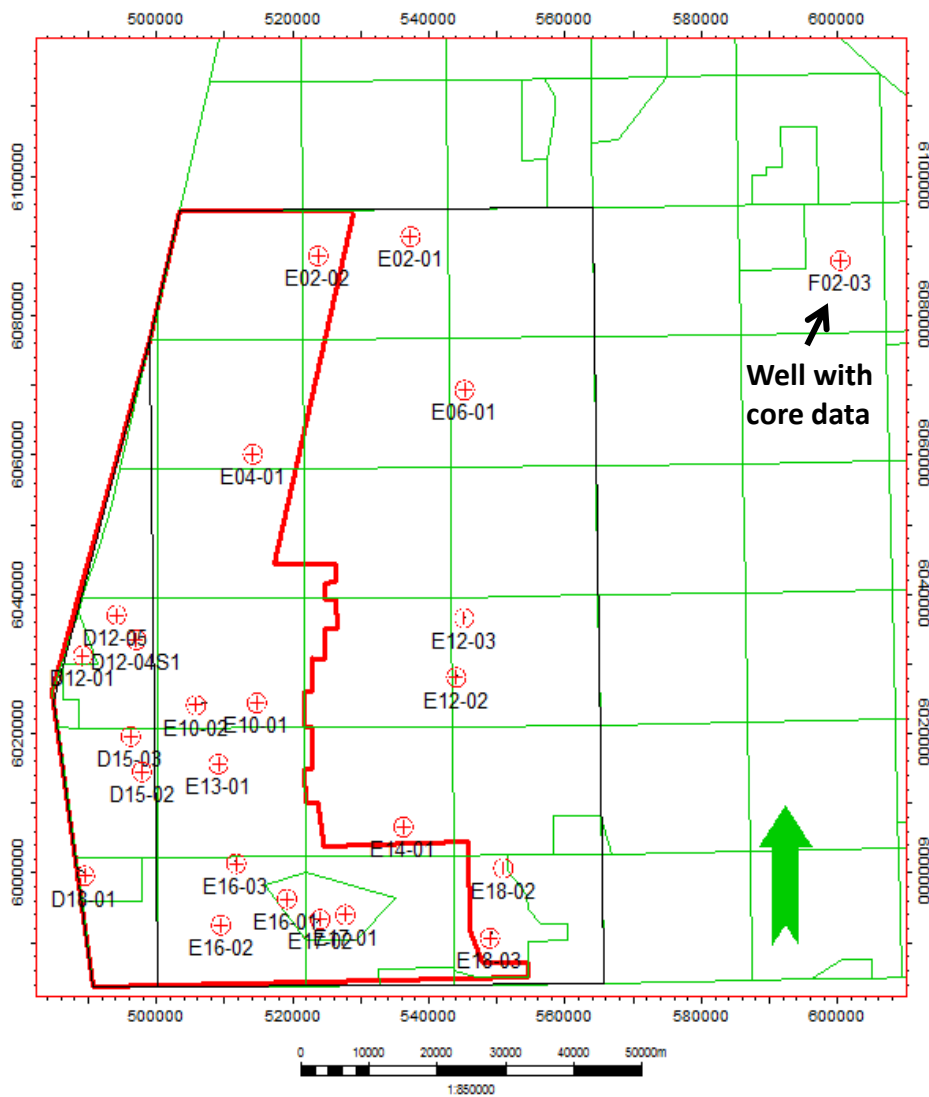


Fig.30) Map showing well data used in this research.

Methods

3.3 Interpretation and visualization tool

The available datasets have been imported in the Petrel software, version 2010.2. This program visualizes the datasets and can be used for geological interpretation. The interpretation of seismic data is based on the continuity and shapes of seismic reflections. Seismic reflections represent sedimentary layers, which become visible due to lithological differences between the layers. These reflections are related to acoustic impedance changes, which are a function of density and velocity in the sediments involved. The seismic reflections are interpreted to construct 3D surfaces for further analysis and interpretation. Visualization of these features can be enhanced via various volume- and surface attributes.

3.3.1 Constructing maps

Surfaces of the most important lithostratigraphic subdivisions in the Dutch subsurface have been imported from the TNO database. However, these maps have been interpreted on a large scale ignoring small structures and therefore some of the maps have been reconstructed for detailed analysis in this research (table.2). These maps have been generated via the 3D auto-tracking algorithm in Petrel. This algorithm automatically constructs a detailed horizon, however sometimes manual improvements have been made where necessary. The TWT thickness maps for the various stratigraphic sequences have been generated by subtracting the top surface from the bottom surface.

Table 2) TWT Maps used in this research

Abbreviation	Name	Maps supplied by TNO	Maps constructed
NU	Mid Miocene Unconformity	x	x
N	Base Tertiary	x	x
CK	Base Chalk	x	x
KN	Base Rijnland	x	
S	Base Schieland	x	
AT	Base Altena	x	
RN	Base Upper Germanic Trias	x	
RB	Base Lower Germanic Trias	x	
ZE	Base Zechstein	x	

The time surfaces constructed in this study are also used to visualize other parameters via surface attributes (amplitude map) and volume attributes (variance map). These parameters were extracted and displayed on top of the interpreted surface.

The surface of the Mid Miocene Unconformity (MMU) has been smoothed to generate a “fault throw map” (fig.51). The surface is smoothed iteratively multiple times until it resembles an almost flat surface at which the smallest structures have been eliminated. This surface can then be used to calculate the “throw values” of the faulted MMU, by subtracting the original surface from the smoothed surface. The created surface gives a good approximation of the actual throw values in the research area, as can be seen from the manual polygonal fault throw measurements (fig.50) compared to the generated fault throw map in fig.51B.

3.3.2 Time-depth conversion

Well data is tied to interpreted surfaces in Petrel. The vertical scale of the 3D seismic data volume is two-way-time (TWT) in milliseconds. However, the vertical scale of well data is given in meters depth and therefore a time-to depth conversion needs to be applied. For some wells check-shot data was available, whereas other wells had to be converted via calibrated velocity logs from TNO (<http://nlog.nl>). Check-shot data represent measurements of the TWT from the surface to a known depth by lowering geophones in the borehole.

In this research time-depth conversion is particularly important for Cenozoic sediments, as in this sequence the mounded structures and polygonal faults have been identified. The obtained velocity data from the wells in the D- and E quadrants give rise to ~2000 m/s for Cenozoic sediments, indicating that TWT in milliseconds corresponds to depth in meters. Cameron et al (1993) identified a similar value for Late Cenozoic sediments in the central and eastern parts of the Southern North Sea.

3.4 Measurements for quantitative analysis

Measurements on polygonal faults, and the mounded structures found on the Mid Miocene Unconformity, have been made for quantitative analysis. The measurement methods are briefly described below.

3.4.1 Measurements on mounded structures

For all the mounded structures, maximum throw of the polygonal faults beneath them, as well as the structural relief of the mounds have been measured assuming zero phase seismic data (fig.31). The term “mound” is used here as a positive relief structure found on top of this unconformity. The structural relief is defined as the height of the mound from a reference level, to measure the actual topographic height. The maximum throw has been measured by placing the seismic intersection perpendicular on the fault in planview (fig.31). Finally the structural relief is plotted against the maximum throw values to investigate if a relationship exists between these parameters.

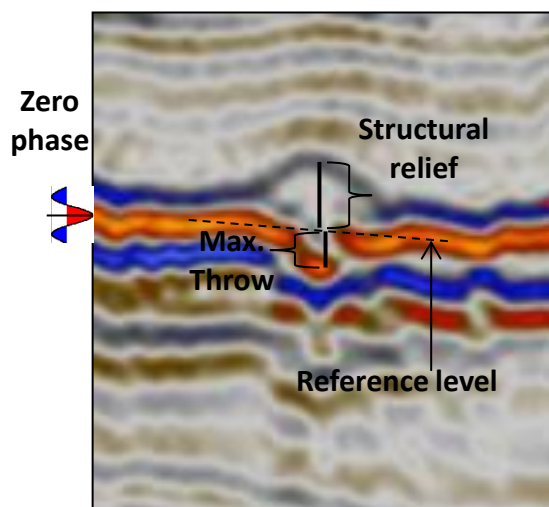


Fig.31) Measurements done on mounded structures (vertical exx. 5x)

3.4.2 Measurements on polygonal faults

In Petrel, polygonal faults can be visualized in different ways, such as in amplitude- or variance maps and ant-tracking cubes. Amplitude maps can be used to visualize subtle differences in seismic amplitude values, for example to detect polygonal faults. The variance attribute gives a value between 0 and 1 for these amplitude differences between a point and the points closely around it. This enables accurate visualization of features such as channels, faults or bodies with chaotic internal reflections, for example chimneys and pipes. The ant-tracking process further clarifies, for example the variance attribute, by identifying and enhancing large amplitude differences e.g. discontinuities. This method can be used for extracting faults from a 3D seismic cube.

During the course of this research several methods have been tried to execute automatic measurements of azimuth, throw and fault length on polygonal faults. The automatic fault extraction tool in Petrel was used for this and constructs faults by fitting fault planes through detected discontinuities. However, the problem encountered with this method was that the algorithm of the extraction tries to link discontinuities together in straight lines, similar to tectonic faults, whereas polygonal faults radiate in all directions.

Also, the RDR structural and fault analysis tool has been tested to perform automatic polygonal fault measurements. The edge-detection attribute available in this Petrel plug-in shows almost similar results as the variance attribute and was therefore not used in this research.

Both these methods did not give accurate values for the interested polygonal fault characteristics and therefore interpretation on the faults has been done manually.

Manual measurements on the faults comprise azimuth, throw and fault trace length. The faults have been measured in two areas of 21 km² (fig.32 & 44) and measurements can be found in Appendix C. These areas comprise a northern area with mounds (blue outline) and a southern area without mounds (red outline). The two areas are used to investigate if differences exist between the polygonal fault characteristics and to investigate a possible relation with overlying mounded structures. The measurements are based on the variance attribute map, which resembles the polygonal faults in the most accurate manner. Interpretation is based on identification of the faults on “tracing paper” in the two areas.

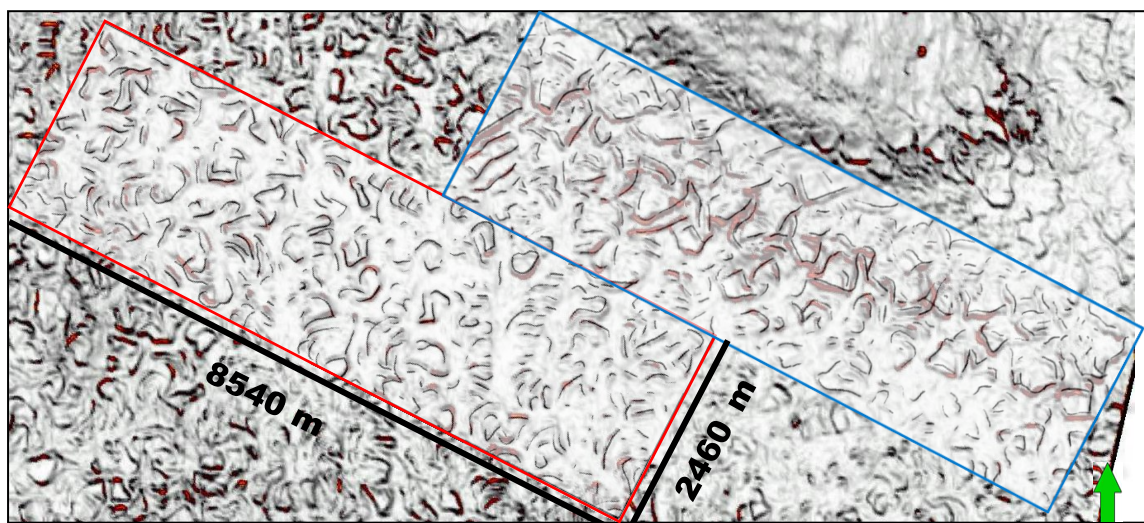


Fig.32) Variance map showing the two polygonal fault measurement areas. Polygonal fault interpretation covers both areas (transparency 40%) Blue outline; area with mounds. Red outline; area without mounds.

In Petrel the length of 40 polygonal faults is measured manually as well as on paper. These measurements have been used to construct a conversion factor for the remainder of the faults in Petrel (Appendix C). The faults with a trace length smaller than ~200 meters, have not been taken into account for further measurements, because small faults do not allow accurate azimuth measurements using this method. The faults larger than ~200 meters have been straightened, since most polygonal faults tend to be curved in planview, for accurate azimuth and length measurements.

Fault throws have been measured for 40 faults in each of the two areas (Appendix C). Not all of the faults have been measured due to the difficulties of the measurements because of seismic resolution limitations. Therefore, only faults which are clearly visible on seismic cross sections, as well as on the variance attribute map, have been used for these measurements (fig. 33).

Finally, the measurements on the polygonal faults have been analyzed to investigate if significant differences exist between these parameters in both areas. These differences are used to investigate if a relationship exists between the polygonal faults and overlying mounded structures.

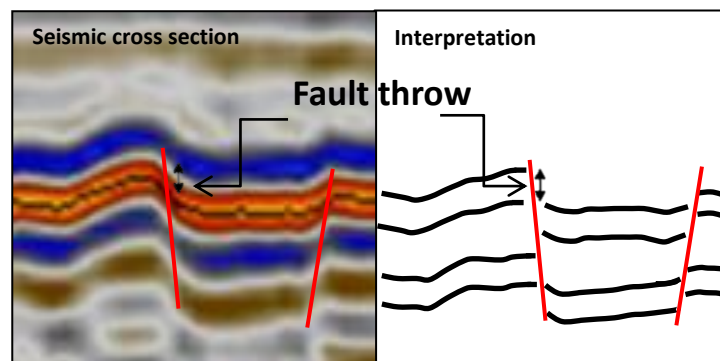


Fig.33) Manual measurements done on polygonal fault throws in (left) seismic cross section (vertical exx. 5x) (right) interpretation

4. Observations and results

In this research, several fluid escape features have been observed in Tertiary sediments of the northern Dutch offshore. This thesis focuses on the polygonal faulting in the Paleogene sediments, as well as the mounded structures found on the Mid Miocene Unconformity (MMU). The first part of the observations describes the mounds. The Mid Miocene Unconformity is the strongest marker in the Tertiary sediments and represents a large unconformity, which can be followed throughout the North Sea (Huuse & Clausen, 2001). The depth of the MMU in the focused study area ranges from -350 ms in the southwest to -950 ms in the northern part (fig. 34).

The second part of the observations comprises the polygonal faults, which have been observed throughout the Middle- and Lower North Sea Groups. These faults are found up to the Mid Miocene level.

The final part of this chapter comprises the results of the quantitative analysis of the polygonal faults. Fault measurements include azimuth, throw and fault trace length for the polygonal faults of the Mid Miocene Unconformity in two distinct areas (fig.43 &44) This has been done to see if differences exist between the polygonal fault characteristics and to investigate a possible relation with overlying mounded structures

4.1 Mounded structures

In the Miocene sediments of the Dutch D- and western E quadrants (~4000 km²) a total number of 135 mounded features have been identified and mapped (fig.34 and Appendix B). The mounded structures have all been identified on the Silverpit- and Cleaverbank platform and can primarily be found at the flanks of salt domes (fig.34). The mounds are found in groups as well as individually, where the grouped mounds are generally found near the salt domes and the individual ones are found further from the domes (fig. 34).

The thickness maps for the Paleogene, Late Cretaceous and Early-Middle Triassic sedimentary packages underlying the mounds, do not appear to relate to the distribution of the mounds. The mounded structures can be found overlying both thick sedimentary sequences, as well as thinner sediment packages (fig. 35 A,B,C). However, the Late Permian Zechstein map does show an influence, as the mounds are generally observed in the vicinity of salt domes (fig.35D). In other areas of the northern Dutch offshore, salt domes are also present (Geluk et al, 2007), however these do not show similar mounded structures at the MMU, with the exception of quadrants G-10 and G-13 (fig.38) (this study).

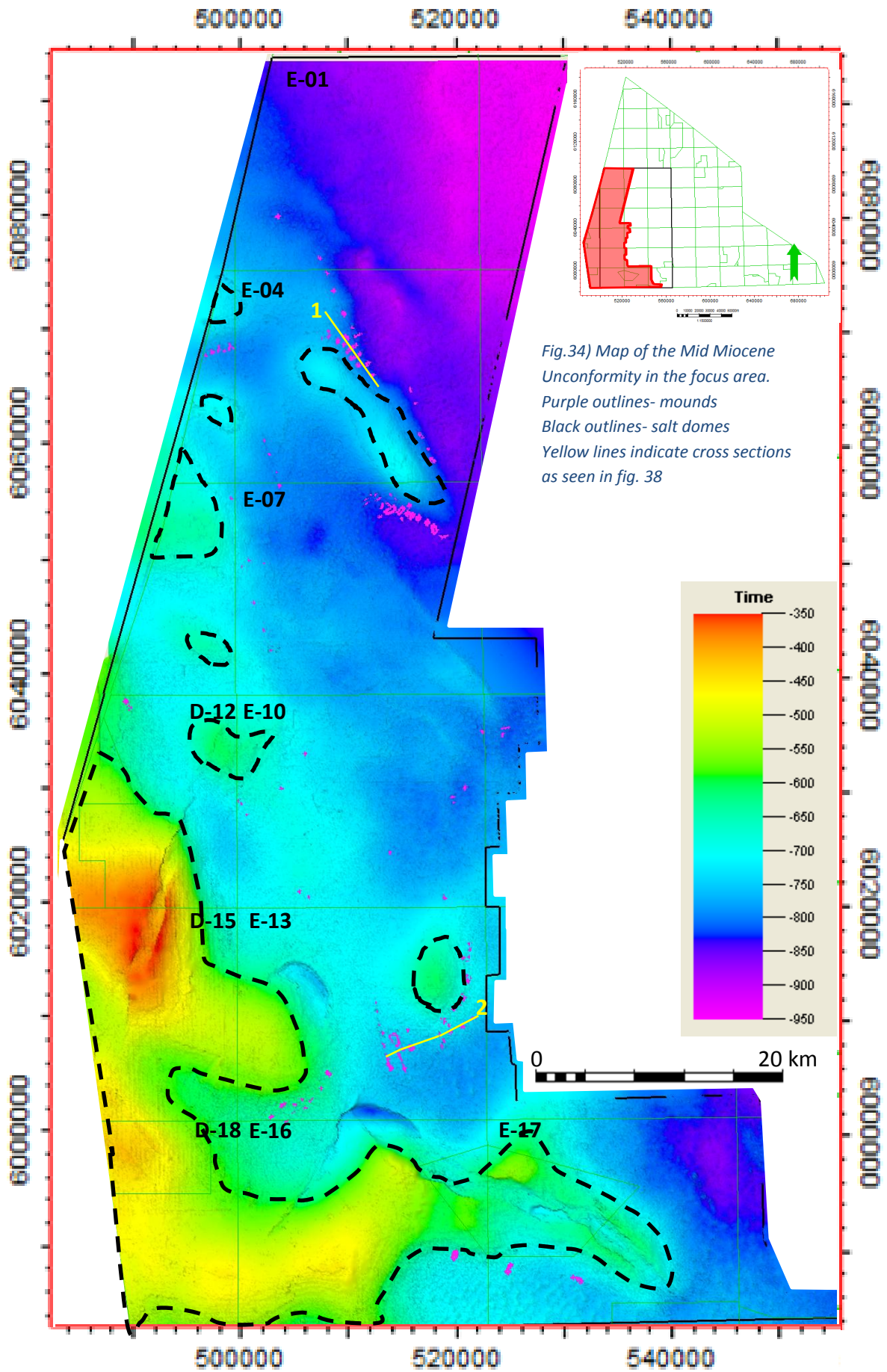


Fig.34) Map of the Mid Miocene Unconformity in the focus area.
 Purple outlines- mounds
 Black outlines- salt domes
 Yellow lines indicate cross sections as seen in fig. 38

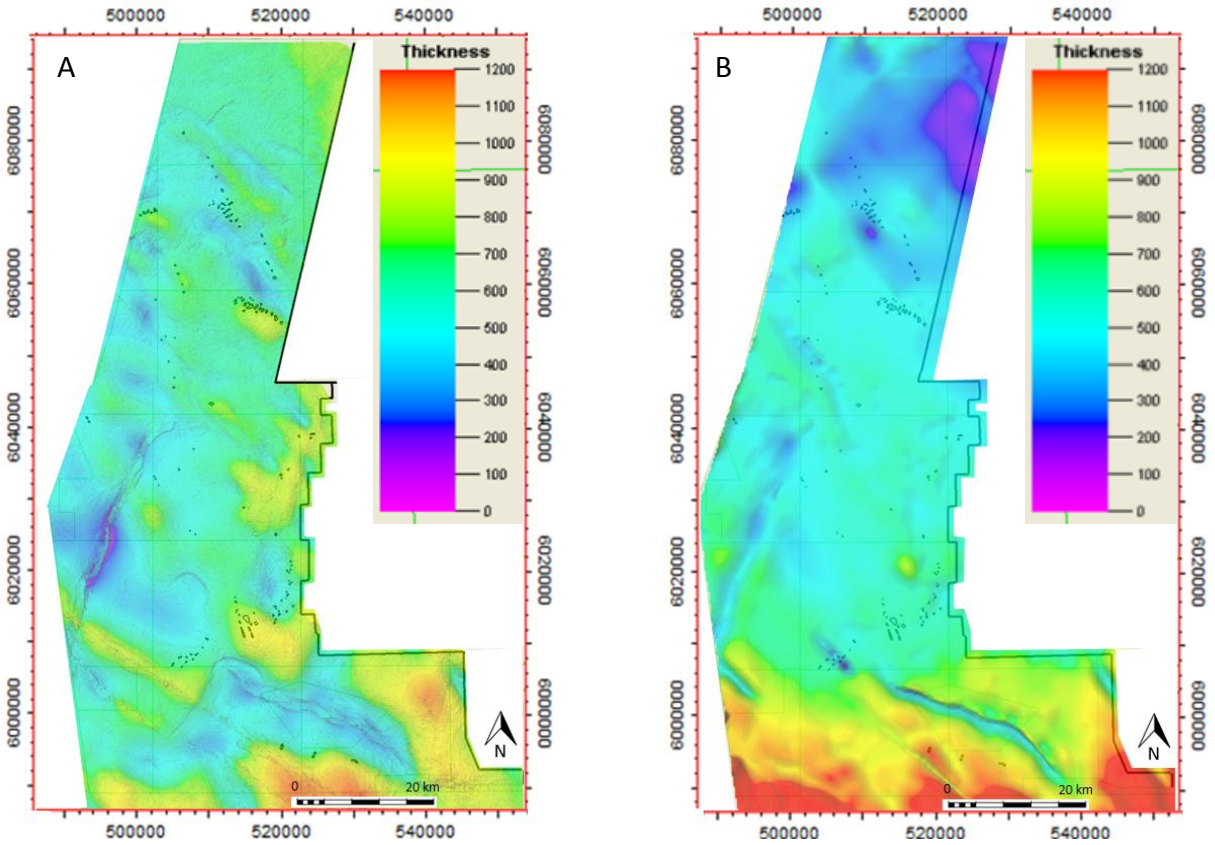
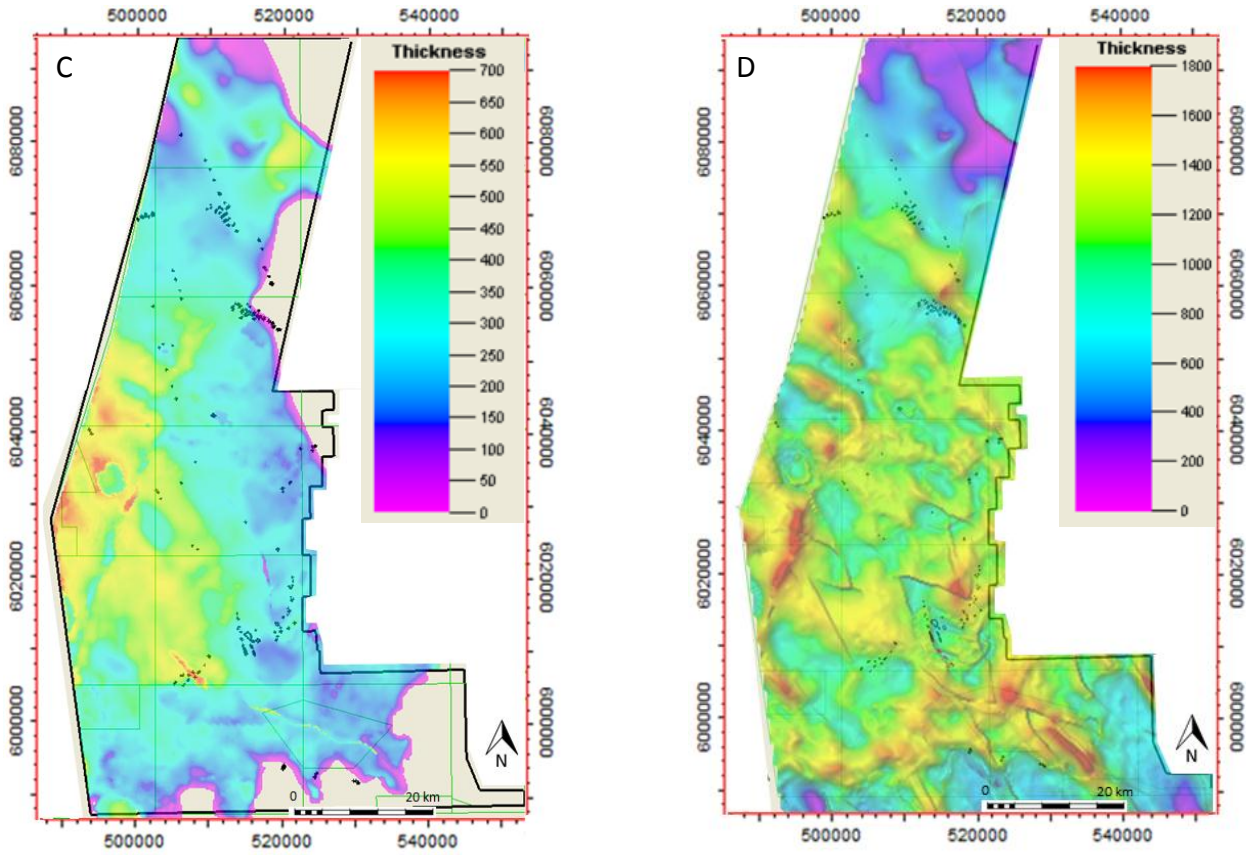


Fig.35 Thickness maps of the study area. Black outlines indicate mounds. A) Lower- and Middle North Sea group (Paleogene) thickness. B) Chalk group (Late Cretaceous). C) Upper- and Lower Germanic Trias group (Early-Middle Triassic). D) Zechstein group (Late Permian)



4.1.1 Seismic character

On seismic cross sections the mounds are recognized as conical structures found on top of the Mid Miocene Unconformity, a negative graben relief beneath it and a “lens- shaped” internal architecture (fig.36 & 37). The majority of mounds do not show internal layering on seismic data. However when visible the internal reflections are generally parallel to the top reflection (fig.37). Some of these reflections progressively downlap on to the base reflection of the Mid Miocene Horizon. In this study mounds with similar layering have also been found in the G blocks of the Dutch Offshore (fig. 38). Occasionally onlap on the mounds can be observed, however sometimes this is difficult to see due to seismic resolution limitations (fig.38.2). The acoustic impedance contrast between the mounds and overlying layers is weak, compared to the Mid Miocene unconformity (fig.38.2).

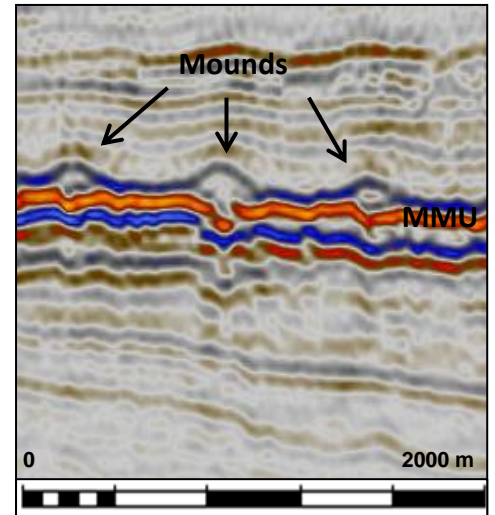


Fig.36) Example of mounded structure as seen on seismic cross sections (vertical exx. 5x)

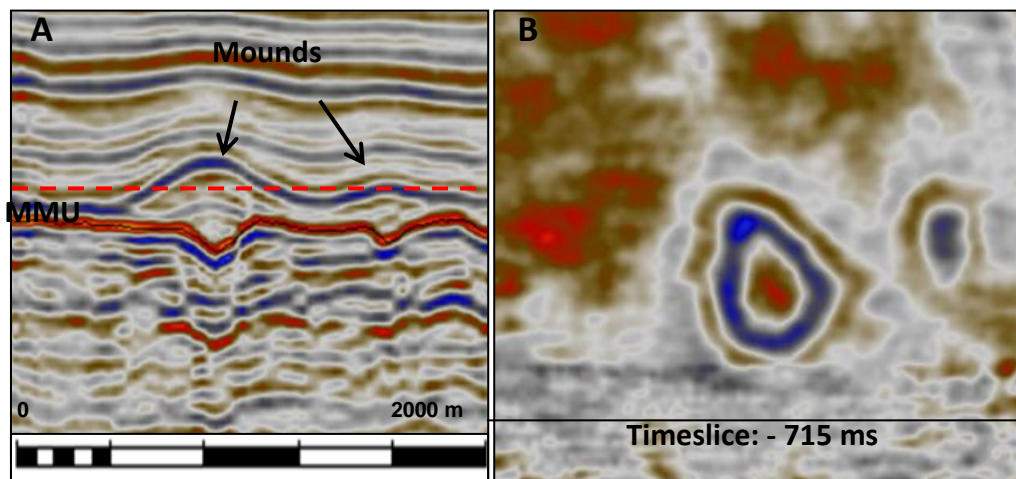


Fig.37) Example of mounded structure with internal layering as seen on A) seismic cross sections (vertical exx. 5x) B) time slice through the mound as indicated in A

The mounded structures sometimes affect the seismic character of surrounding reflectors. This can be seen as a velocity pull-up below the mound, which represents an apparent uplift produced by a local, shallower high-velocity region, or a “draping of sediments overlying the mounds, which is caused by differential compaction between the mound and overlying sediments (fig.38) (Andresen et al, 2009).

Another observation that sometimes is identified comprises a vertical disturbance e.g. “blurring” of reflectors directly underlying the mounds, which might result from ascending fluids and/or hydrocarbons (fig.38.1) (Loseth et al, 2009).

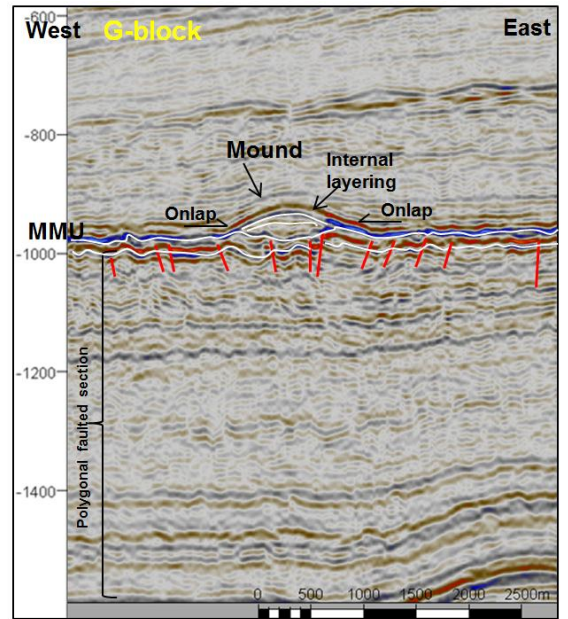
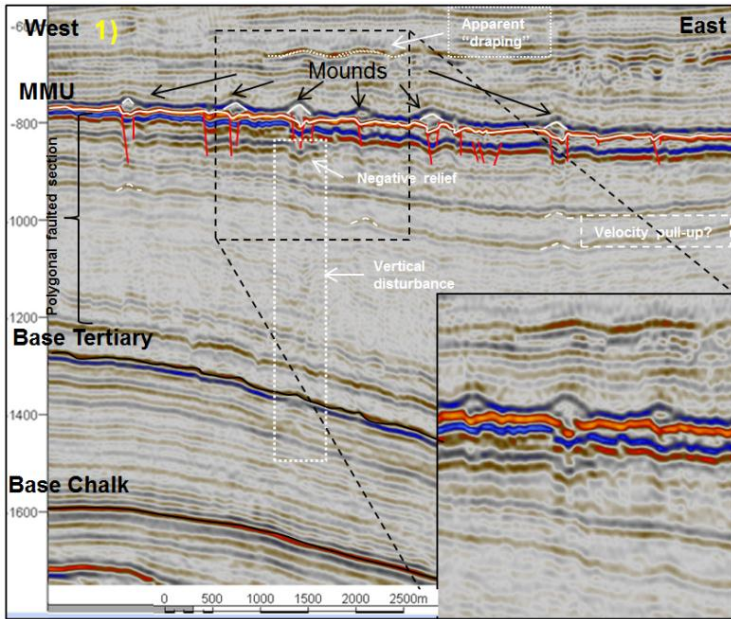
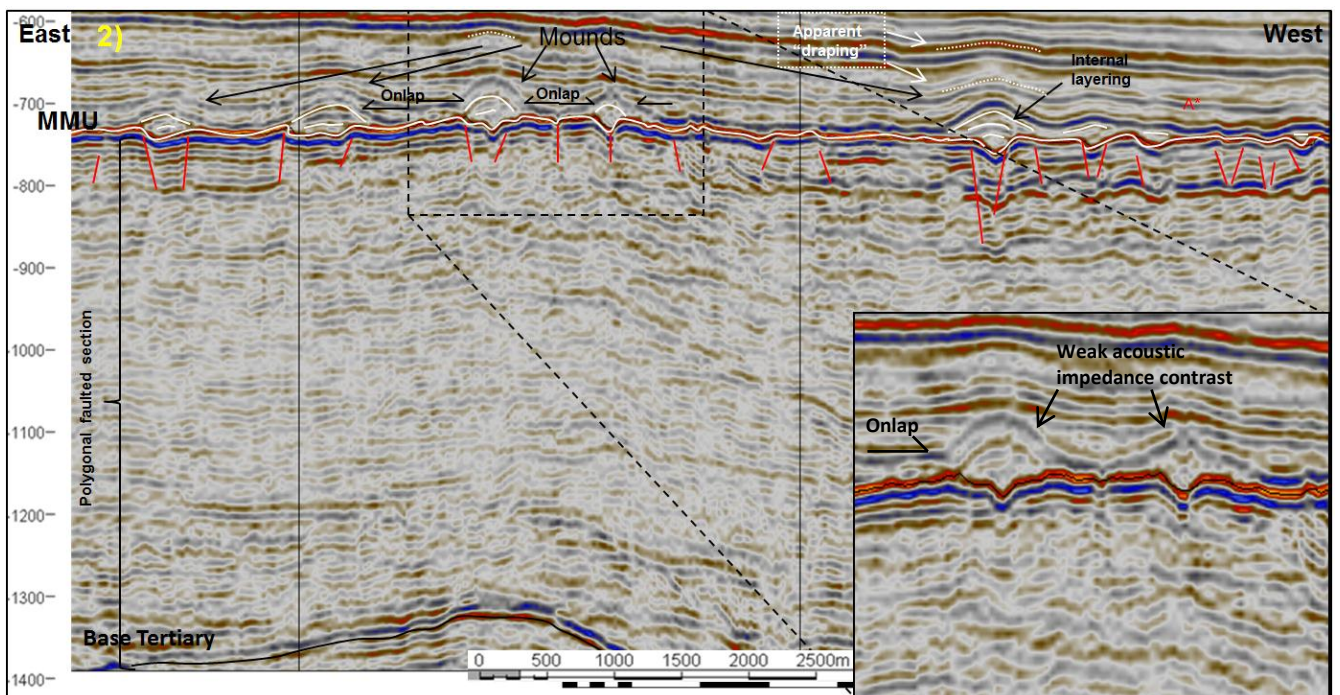


Fig.38) Cross sections through mounded areas as indicated in fig.34 and observed in the G-block (vertical exx. 5x)



4.1.2 Geometry

Shapes of the mounds in planview are usually circular for individually occurring mounds, to elliptical or elongated for grouped mounds. The elongated grouped mounds are generally orientated towards the salt domes.

The diameter of the mounds ranges from a few tens of meters up to kilometer scale for elongated structures. The height of the mounds is measured as the structural relief and ranges up to 35-40 m (fig.39). The majority of the mounds range in size from 16 to 26 m, after which the values decrease rapidly. The smallest mounds (< 12 m) have not identified on seismic data due to resolution limitations.

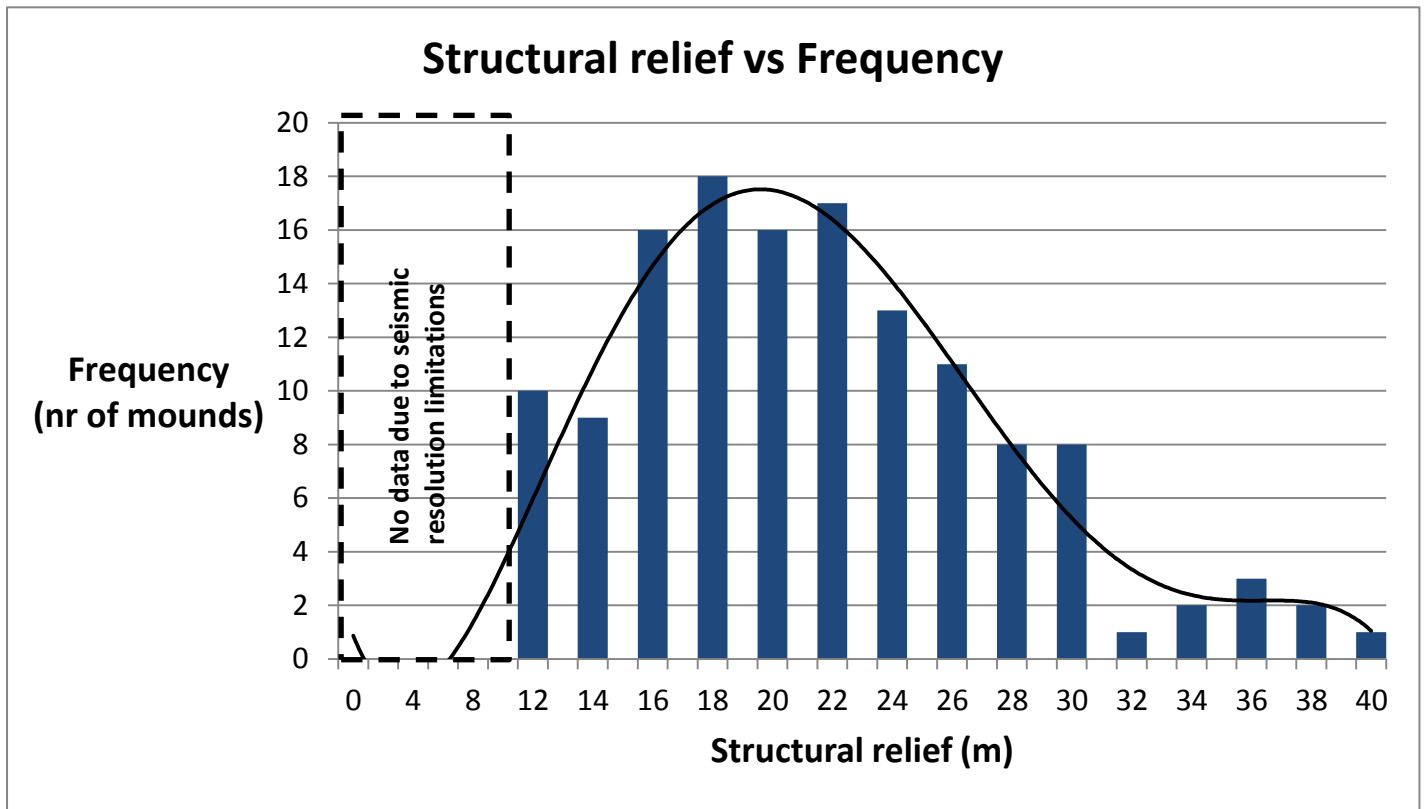
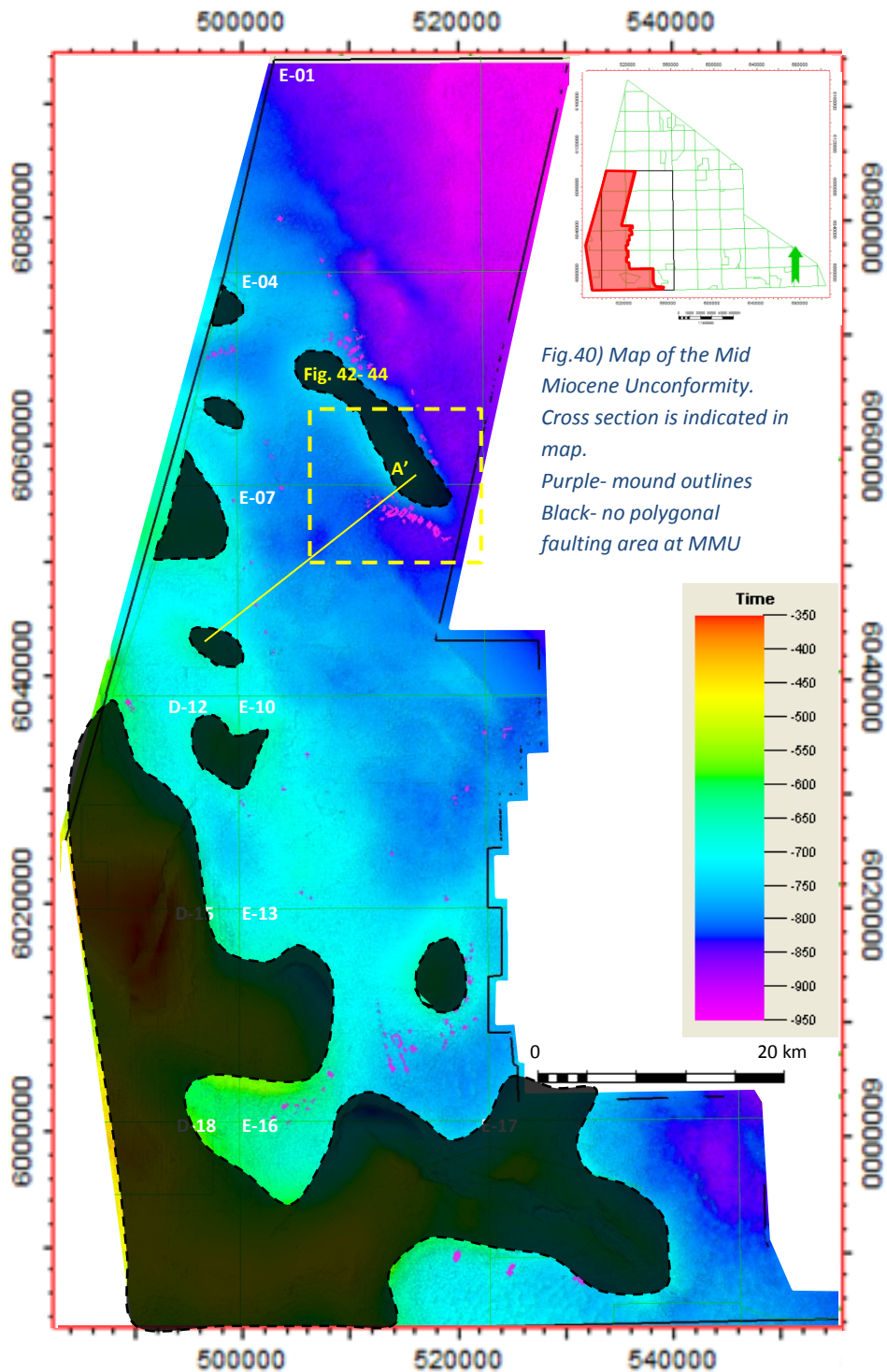
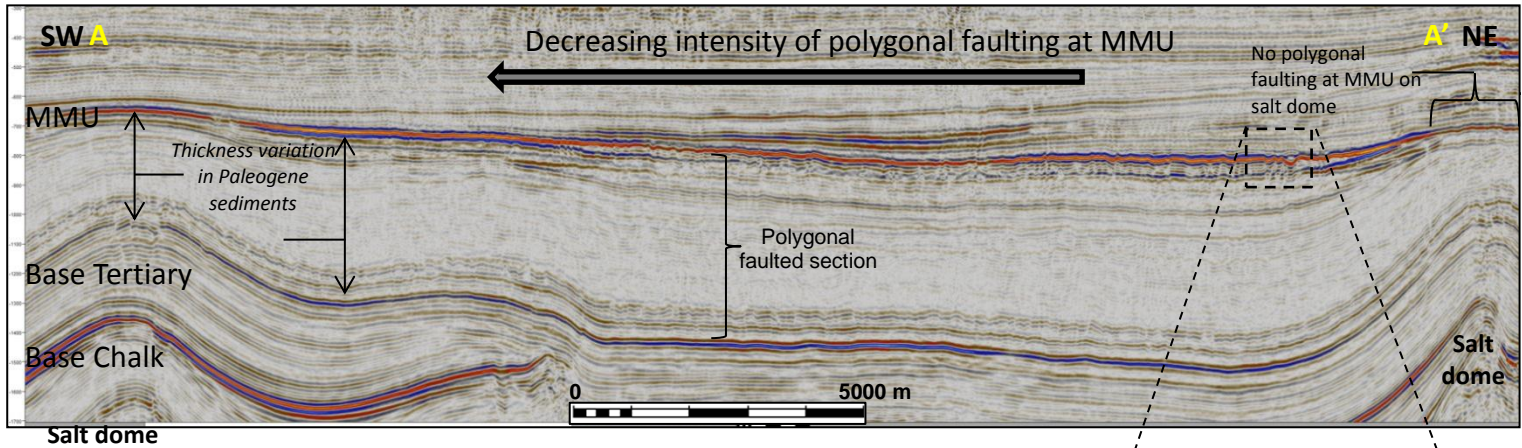


Fig.39) Plot of mound measurements showing the structural relief vs frequency of mounds (n=135)

4.2 Polygonal faulting

Polygonal faulting has been identified throughout the northern Dutch offshore blocks A- to G. These small, extensional faults have only been observed in the Paleogene mudstones of the Lower- and Middle North Sea group and terminate at the Mid Miocene Unconformity. This polygonal fault system has previously been identified in the Central North Sea as well (Cartwright et al, 1994). In the focus area polygonal faulting at the MMU appears to decrease in intensity towards the southwest and above salt domes (fig.40). Another clear observation is that mounds have only been identified in areas where the Mid Miocene Unconformity is polygonally faulted (fig.40).





4.2.1 Seismic character

The polygonal faults are identified on seismic cross sections as layer-bound extensional faults, with a small offset (< 20 meters). Some of the faults can be correlated downward, but for most faults this is difficult to interpret due to resolution limitations (fig.41).

In planview these faults can be visualized in different ways, including in amplitude and variance maps (fig.42A &B). However, these maps do not show similar fault patterns, and therefore quantification of the faults remains difficult. The sizes of the fault polygons can range up to hundreds of meters, and these do not show the classical regular hexagonal pattern (fig.42 A&B). Furthermore the fault polygons are not always closed and sometimes smaller faults are found inside larger polygons (fig.42C).

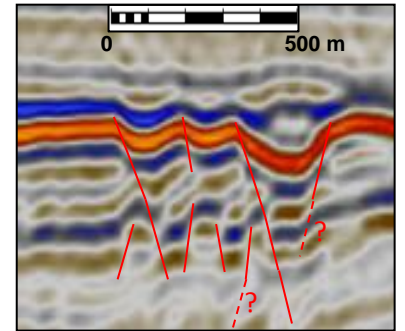


Fig.41) Polygonal faulting as interpreted on seismic cross sections (vertical exx. 5x)

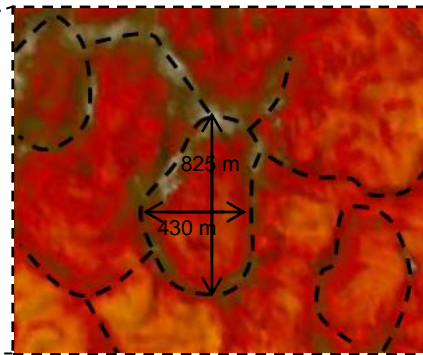
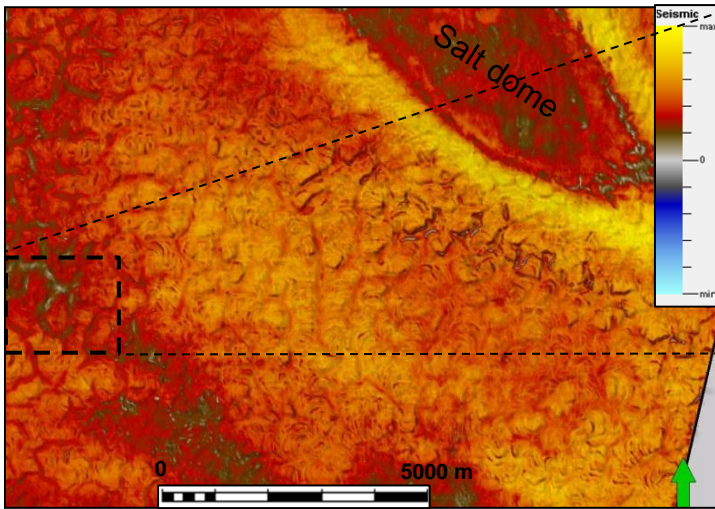


Fig.42A) Left: Amplitude map of polygonal faulting visualized on top of the Mid Miocene Unconformity. Above: dashed lines: fault interpretation on amplitude map

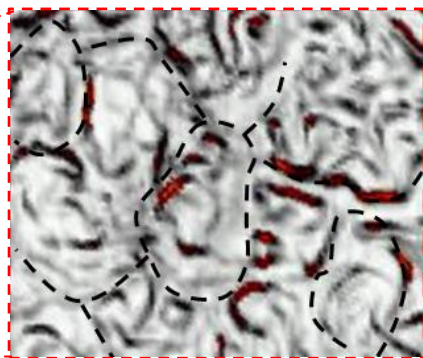
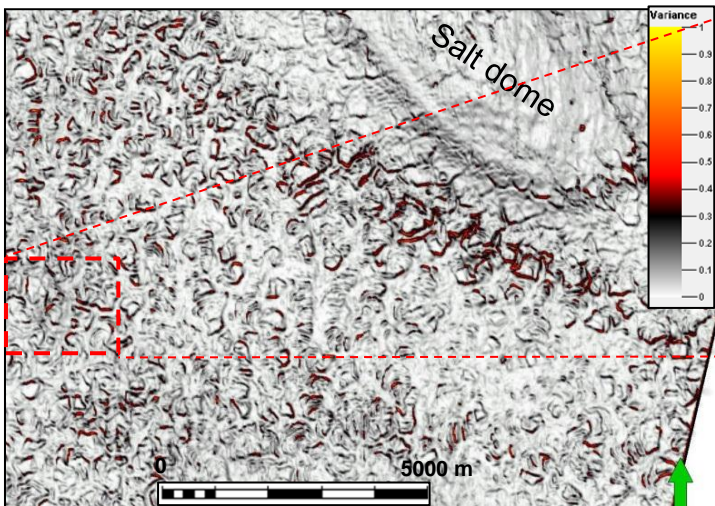


Fig.42B) Left: Variance map of polygonal faulting area visualized on top of the Mid Miocene Unconformity. Above: dashed lines: fault interpretation based on amplitude map

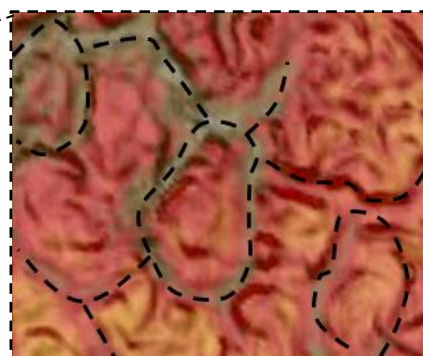
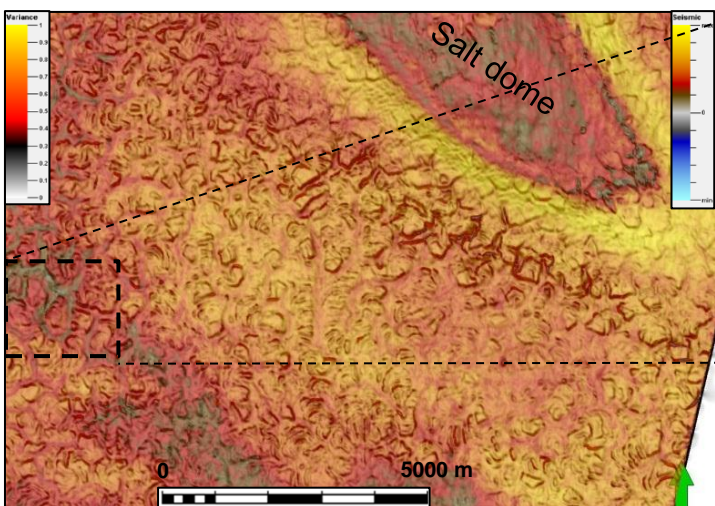


Fig.42C) Left: Combined map of variance and amplitude attributes visualized on top of the Mid Miocene Unconformity. (transparency 50%). Above: showing the difficulties associated with polygonal faulting quantification (smaller faults can be found inside larger fault polygons)

4.3 Quantitative analysis on polygonal faults and mounded structures

This part of the results comprises a quantitative analysis of the polygonal faults measured in two areas of 21 km² each (fig.43). These areas comprise a northern area with mounds and a southern area without mounds (fig.43-46). Manual measurements comprise 205 faults in the no mound area, and 175 faults in the mound area (fig.44). The measurements are used to see if differences exist between the polygonal fault characteristics and to investigate a possible relation with the overlying mounds. Polygonal faults can act as migration pathways for ascending fluid and/or sediment mixtures, and are therefore able to create these structures (Hansen et al, 2005; Cartwright et al, 2007).

An important observation is that the mounds generally relate to a horst graben structure with the mounds positioned on top of the grabens (fig. 45). These grabens usually consist of two parallel extensional faults being part of the PFS network, which can be continued deepest in the Middle North Sea Group.

4.3.1 Polygonal fault measurements

Polygonal fault measurements comprise fault trace length, azimuth and maximum throw value. This data can be found in Appendix C.

Azimuth measurements have been divided in classes of 15° for best visualization in the rose diagram, which shows the frequency distribution of the fault set orientation (fig.47). Measured faults radiate in all directions, which is characteristic for polygonal fault systems. However, azimuth measurements on the polygonal faults for both areas do show a weak preferred orientation, as shown in the rose diagram for faults orientated N-S, between N (~330°- 15°) and E-W, between E (~60° and 120°). For both areas faults orientated NW-SE, between N (~300°-330°) show the least number of faults. A similar gap also exists in the no mound area for faults orientated between NE-SW, between N (~30°-60°), whereas this decrease in the mound area is not visible (fig.47B).

The fault trace length versus azimuth plot of fig.48 shows the longest faults to be found between ~45°-75°. These azimuth values closely coincide with values for the salt dome orientation (35°- 57°).

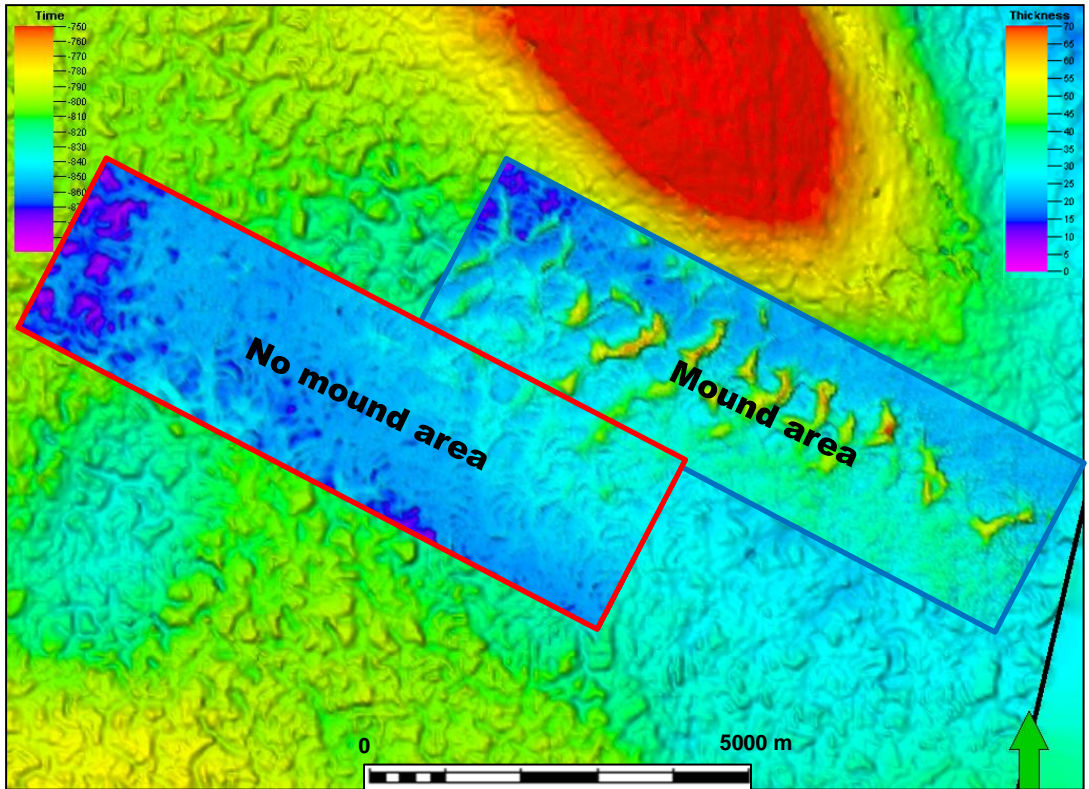


Fig.43) TWT map of MMU, area as indicated in fig 40, (vertical exx. 10x) overlain by the constructed thickness map of the reflector overlying the MMU. The thickness map shows the two areas used for quantitative analysis; Red box- no mound area, Blue box- mound area

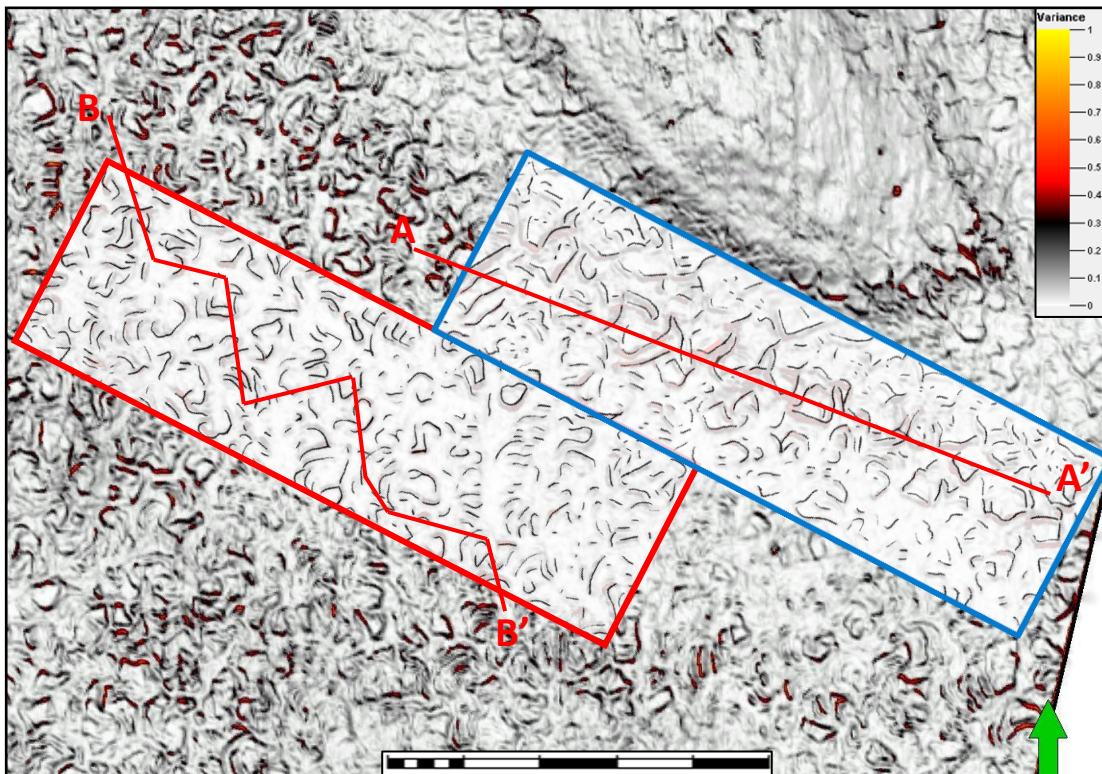


Fig.44) Variance map of polygonal faulting area visualized on top of the Mid Miocene Unconformity (MMU), overlain by fault interpretation maps for the two research areas (transparency 20 %). Including location of 2 cross-sections. Red box- no mound area, Blue box- mound area

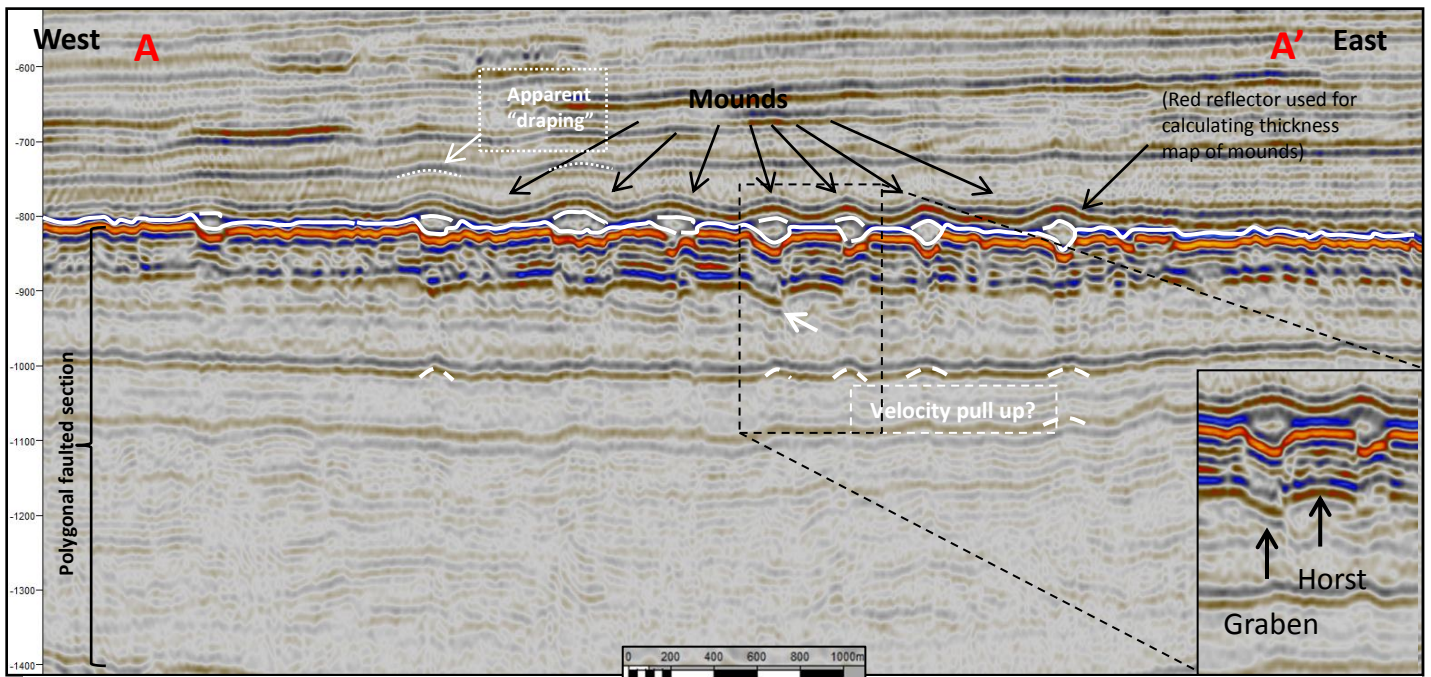


Fig.45) Cross section through mound area, including interpretation (similar as cover page image). See fig.44 for location

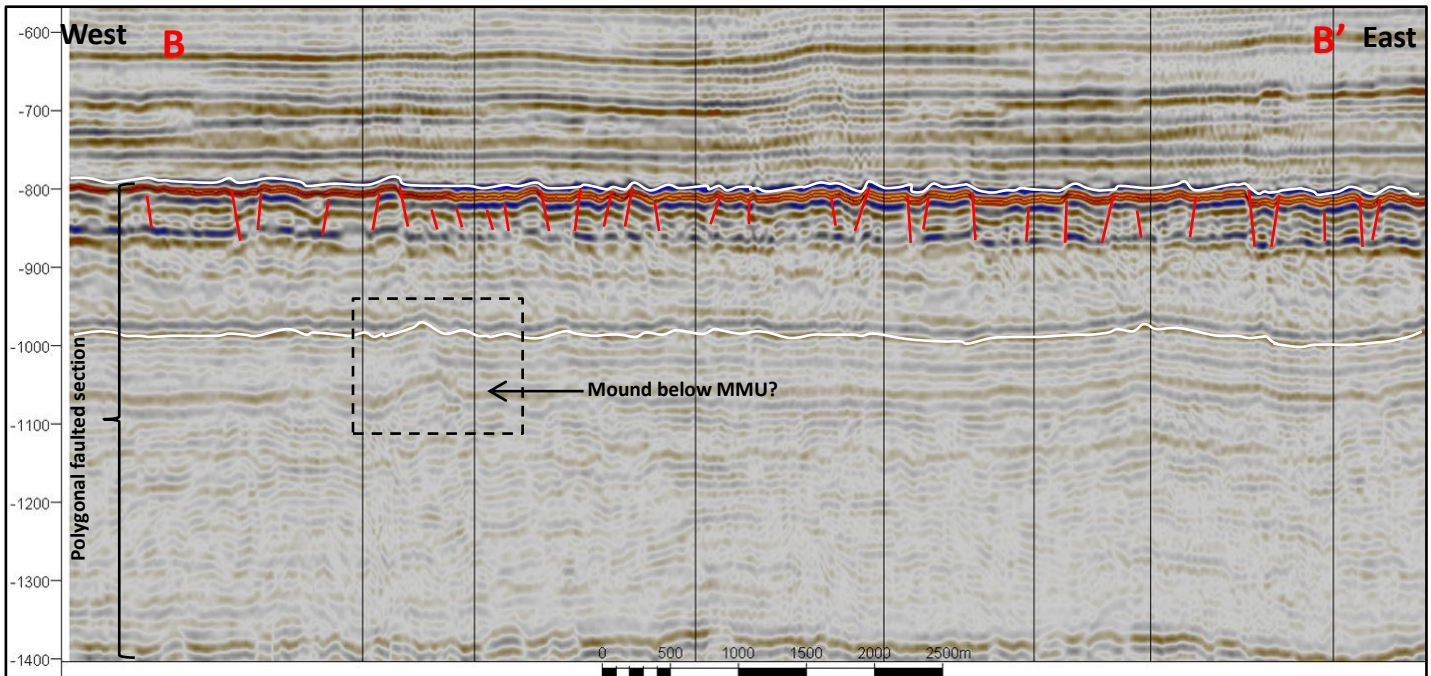
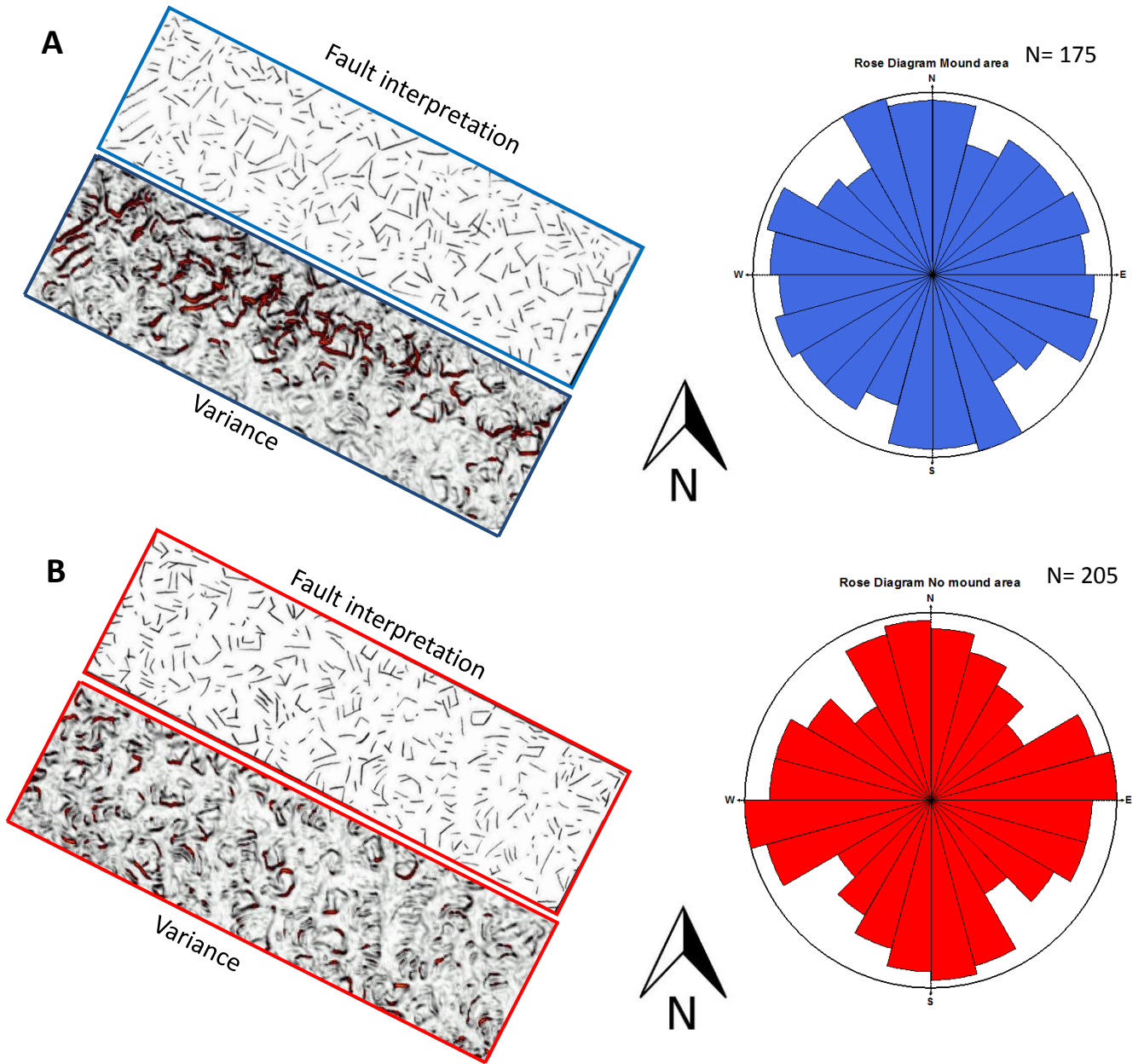


Fig.46) Cross section through no-mound area, including interpretation. See fig.44 for location

Fig.47) Fault interpretation and azimuth measurements for (A) mound area and (B) No mound area



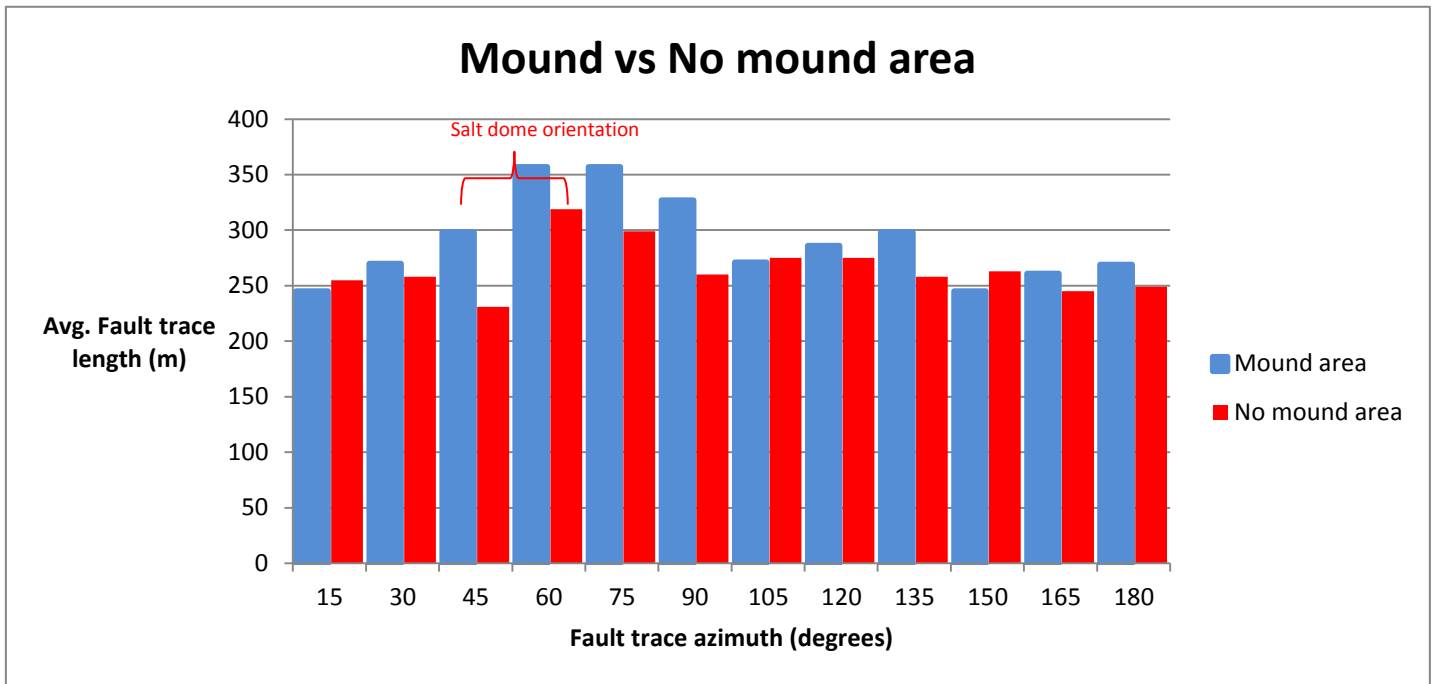


Fig.48) Plot of the fault trace azimuth vs the fault trace length for the Mound area (blue) and No mound area (red)

Fault trace length measurements range from ~200 meters up to ~750 meters in the mound area, whereas the longest fault in the no mound area (N =205) is ~550 meters (fig.49). The mean value the fault length for the no mound is 264 meters (N=205), and for the mound area is 291 (N=175), which represents ~10% increase. The increased fault trace length values can also be seen from fig. 48 for the different azimuth classes of 15°. The scatter plot of the frequency distribution versus the fault trace length, shows that the fault lengths in the no mound area are generally smaller (fig. 49).

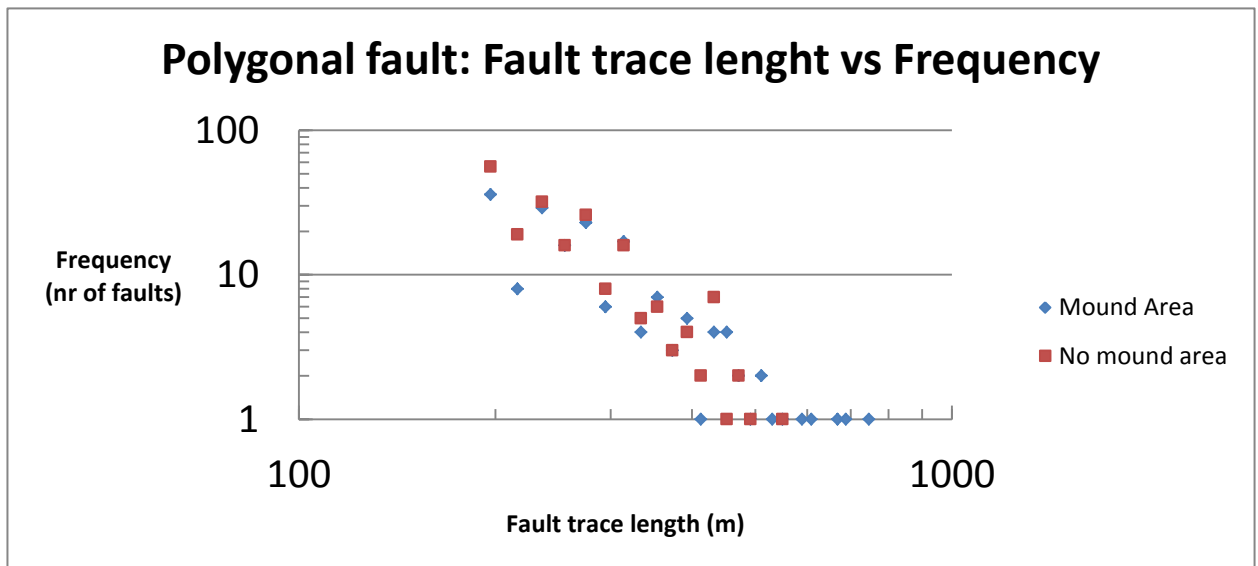


Fig.49) Scatter plot showing the fault trace length vs frequency of total number of faults per area.

Throw values have been measured manually for 40 faults in each area, selected based on visual identification on seismic data. These measured faults can be clearly identified on the variance map, as these show the largest values e.g. closest to 1. The throw measurements indicate generally higher throw values for faults in the mound area, compared to the no mound area (fig.50). The relationship between fault length and throw values results in a shallower slope for the no mound area, compared to the mound area.

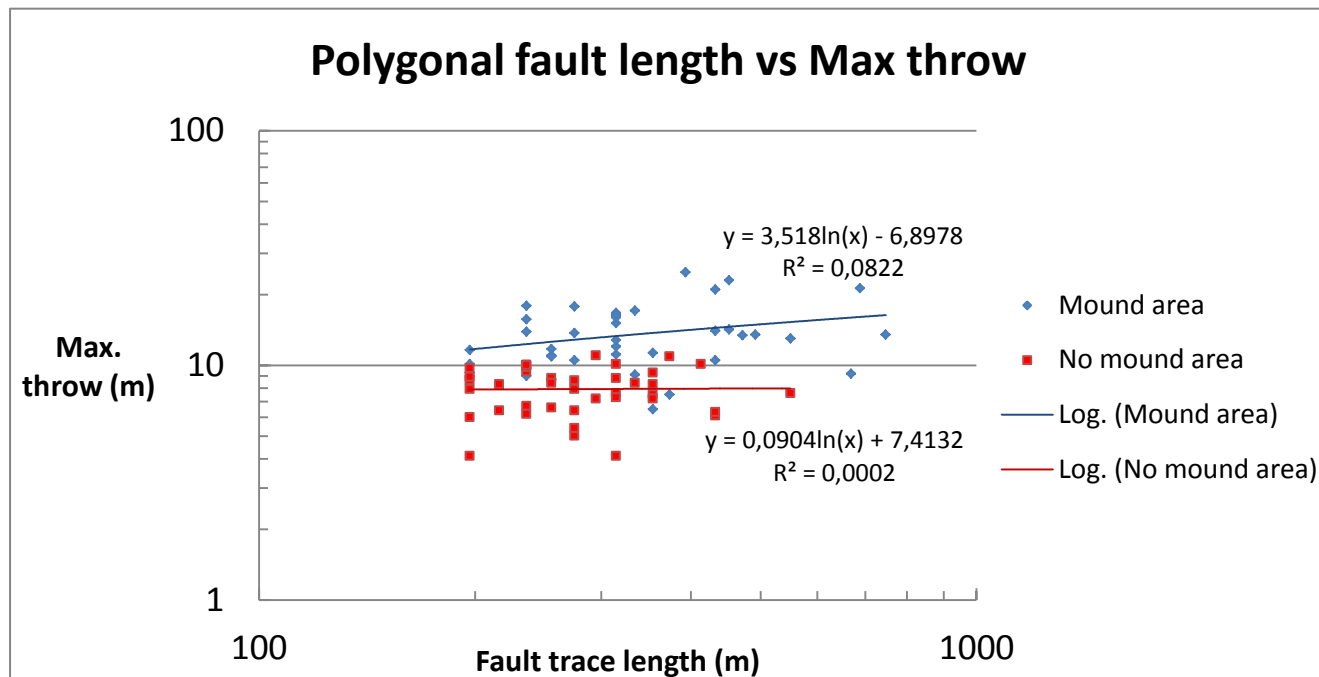


Fig.50) Scatter plot showing the fault trace length vs maximum throw values of faults per area.

Another way to visualize the fault throw is in TWT maps of the Mid Miocene Unconformity in the D- and E blocks, which have been constructed by smoothing the TWT map and subtracting the original surface from the smoothed surface. These constructed maps give a good approximation of the actual throw values in the D- and E blocks (fig. 51). This can be seen in fig.51B where large throw values (> 10 m) generally coincide with mound outlines (purple) in fig.51A. The large throw value area in the top of fig. 51B is caused by an overlying bright spot, which alters the response of underlying reflectors and thereby creating a large value in the constructed throw map.

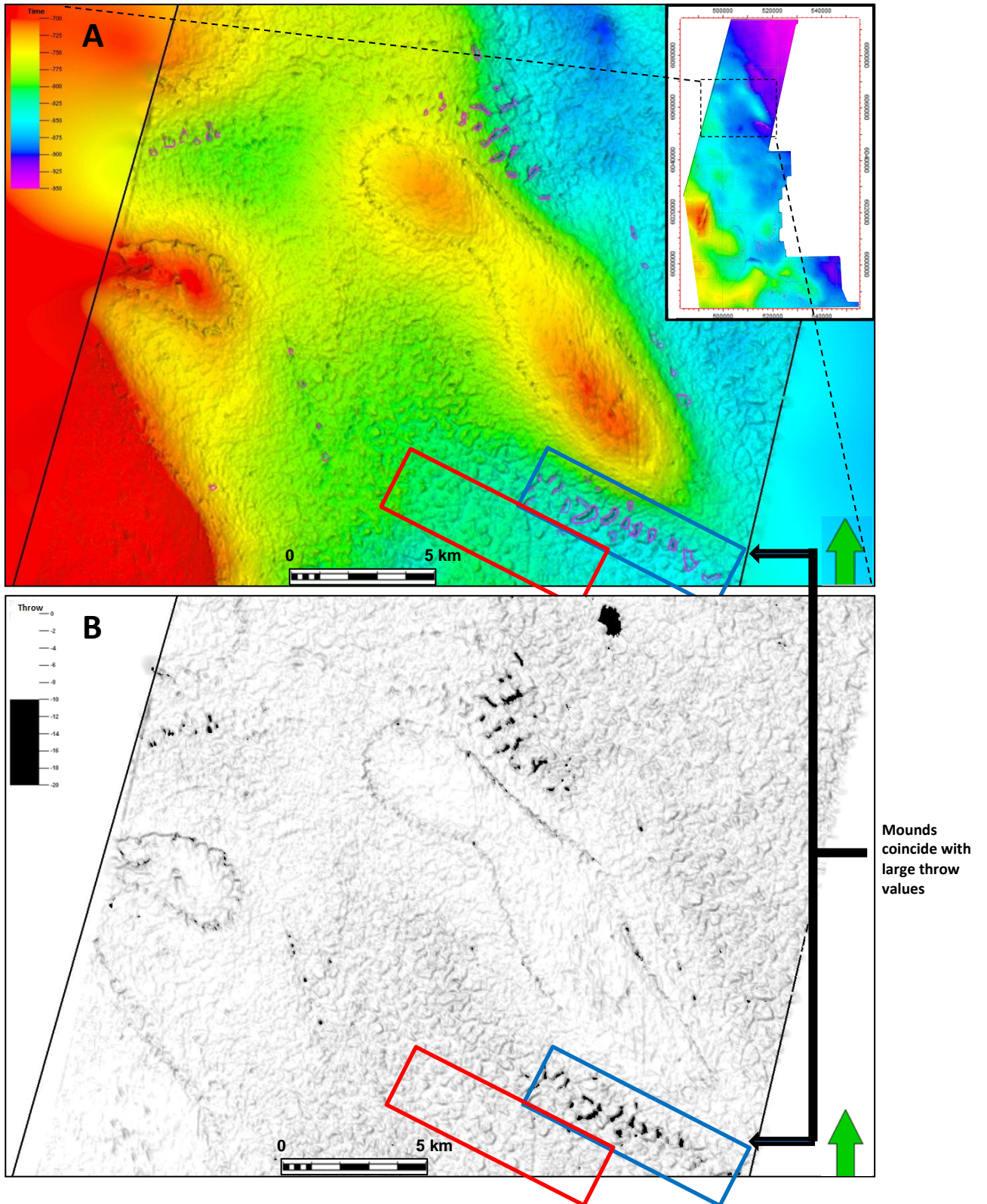


Fig.5.1 a) TWT map of MMU including outlines of mound area(blue) and no mound area (red).Pink - represent mound outlines
 b) Generated TWT fault throw map of area as indicated in fig.5.0a. Black color indicates large fault throw values (>10 m).

4.3.2 Relationship between polygonal faults and mounded structures

The results from the quantitative analysis in the mound and no mound area result in subtle differences in polygonal fault characteristics. According to the results from quantitative analysis of the faults there is a possibility to predict the presence or absence of mounded structures on the basis of these fault characteristics.

Azimuth values only slightly differ between the two areas, and therefore a predictable behavior is difficult to establish for this fault characteristic. Fault trace length values differ between both areas, as longer faults tend to be found in areas with mounds. However, the values do not show significant differences that a predictable behavior can be reached. Throw values do show significant value differences between both areas, as large throw values coincide with mounded areas (fig. 51). The predictable behavior is thus, that there is a higher probability for mound occurrence in regions with large throw values.

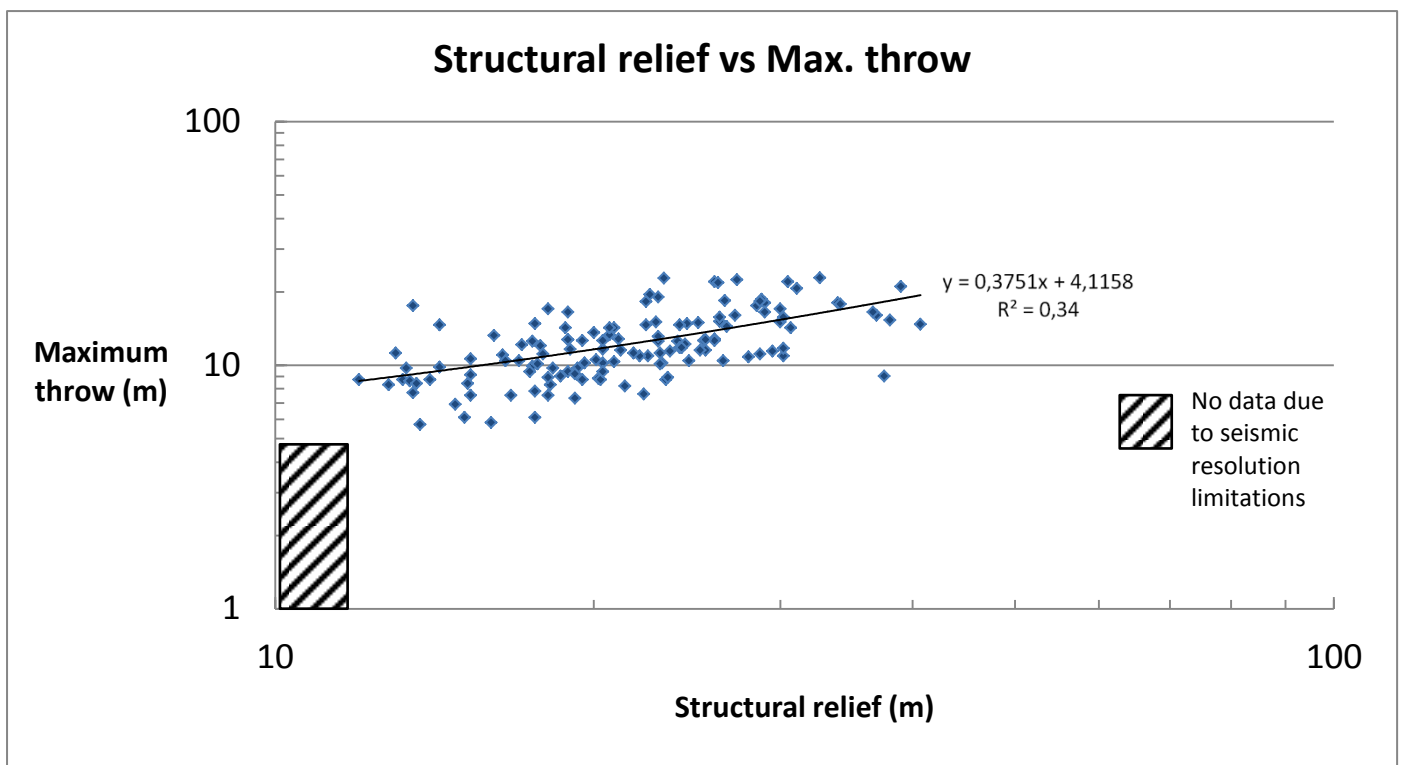


Fig.52) Scatter plot showing the structural relief of the mounded structures (N=135) vs maximum throw of the underlying polygonal faults.

Another correlation which can be found between polygonal fault throw and mounded structures is that the structural relief grows with increased throw values (fig. 52). This plot shows the presence of a positive relation between the height of the mound and the magnitude of the underlying fault throw, which shows the structural relief to be generally larger than the maximum throw values. Furthermore, it appears that the volume of the "additional sediments" in the mounds does not coincide with the volume of "missing sediments" in the grabens (fig. 38.2).

5. Discussion

A number of questions arise about the observed mounds in the D- and E quadrants. These relate to the origin and composition of the mounds, and which factors are influencing the distribution. Furthermore the observed relationship between the mounds and underlying polygonal fault system has implications on the origin of the mounds. In this chapter it is first described which factors are related to the distribution and secondary several options are discussed regarding the mounds' lithology and origin. Finally, the discussion evaluates the results and investigates the possible implications of the mounds and polygonal fault system on the petroleum industry.

5.1 Distribution of the mounds

Based on the observations several factors might influence the distribution of the mounds, these comprise the timing of salt movements and the presence of polygonal faults at the Mid Miocene Unconformity. These factors will briefly be discussed below.

Generally, the mounds are found in the vicinity of salt domes in the D- and E quadrants. Salt domes have been formed by halokinesis, however the timing of halokinesis differs throughout the northern Dutch offshore. The salt domes present in the study area, as well as in the G quadrants, have continuously been moving since Early Cenozoic time. This can be seen from the thickness variations of the Lower- and Middle North Sea group sediments (fig.35A & 40). Whereas in other areas, such as along the Dutch Central Graben, salt has been moving since Triassic time (Geluk et al, 2007). These areas represented sedimentary basins and accumulated a thick sedimentary package in Triassic and Jurassic time, whereas the study area and G-quadrants represented platforms and received little sediment (fig.2). The onset of the salt movements in Cenozoic time could thus have influenced the post-depositional processes affecting the North Sea group sediments, as rising salt domes can push formation fluids forward (Marco et al, 2002). The created fluid flow, might have resulted in an additional factor driving the sediment entrainment in the ascending fluids.

Mounds have only been identified in areas where the Mid Miocene Unconformity is polygonally faulted. On top of salt domes as well as in the southwestern part of the study area, no polygonal faulting is identified at the MMU (fig. 40). Biostratigraphic research indicates that the areas in the southwest were approximately at sea level in Miocene time, and therefore might indicate a higher energy environment (TNO, personal communication, De Bruin). The resulting larger grain sizes may have prohibited polygonal faults to form, as polygonal faults have only been recognized in very fine grained sediments (Gay et al, 2004; Cartwright, 2011). A possible explanation for the absence of mounds on the salt domes might be that these have already been eroded during the Mid Miocene hiatus.

Polygonal faults are formed due to the dewatering of rapidly buried clays of the Lower- and Middle North Sea group (Cartwright, 1994, 2011). The mounds might represent the surface expression of preferential fluid pathways, as they are formed on top of the faulted MMU. Furthermore the height of the mound and the magnitude of the underlying fault throw show a positive relation (fig.51). This strongly suggests that there is a genetic relationship between the mounds and underlying polygonal faults. Perhaps the growth of the faults and mounds is aided by the salt movements, by focusing- and pushing pore fluids out of the Paleogene mudstone sequence.

5.2 Lithology and origin of mounds

No wells have been drilled through the mounds in the study area and therefore interpretation is limited to seismic interpretation and associated amplitude characteristics. The mounded structures can comprise a wide range of rock types including; 1) igneous, 2) salt, 3) carbonate, and 4) siliciclastic rocks (Dahlgren and Lindberg, 2005; Hansen et al, 2005; Andresen et al, 2009, 2010). These different options will be discussed below, and are related to their possible origin.

The first question to be resolved is whether or not these seismic features are true mounds, and not simply represent a relief-feature caused differential compaction. These features are formed by less compactable sediments encased by more compactable sediments, thereby creating “apparent” mounds. The compaction of sediments is related to two processes; mechanical compaction at shallow depths and chemical compaction in the deeper subsurface (> 2-3 km depth) (Avseth et al, 2005).

At deposition the porosity of the encasing North Sea group mudstones can reach values up to 80%, which is caused by the high porous structure of the clay minerals. These values drop significantly during early burial, whereas other sediments such as sand and carbonate having initial porosities up to 40-50%, do not decrease values so rapidly. This difference in compaction rates might thus appear as “mounds” on seismic data. Liu and Roaldset (1994), investigated sands and shales from the Northern North Sea, and constructed an empirical relation between the porosity reduction as a function of depth (fig. 53).

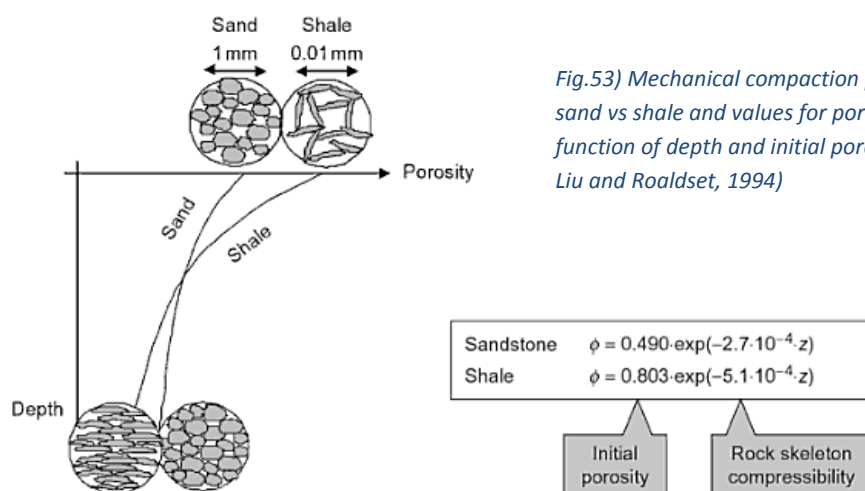


Fig.53) Mechanical compaction process of sand vs shale and values for porosity as a function of depth and initial porosity (from Liu and Roaldset, 1994)

The geological process which could lead to the formation of the mounds first assumes that the less compactable sediments would have been deposited in a depression, otherwise the differential compaction would not be noticed. These depressions could have been formed by polygonal faults reaching the paleo-seafloor.

To reconstruct the structural relief of the mounds unrealistically high compaction values would be needed, as most mounds are observed ~700-850 meters depth. The question remains, how valid the values of the empirical relation for the sediments of the Northern North Sea are compared to this study area. However, an apparent “draping” of some of the layers overlying the mounds is observed (fig.38 & 45). This apparent “draping” directs to a factor of differential compaction (Andresen et al, 2009), possibly contributing to the observed structural relief of the mounds.

The unrealistically high compaction values, combined with the observed onlap on the mounds and presence of internal layering give rise to an actual topographic relief originating on the paleo-seafloor (fig. 38). Therefore the process of differential compaction as origin of the mounds is discarded and the mounds are defined as real structures.

Igneous

According to van Bergen and Sissingh, (2006) igneous features are not present in Cenozoic sediments of the study area, except for the widely distributed Paleogene Dongen tuffite layer. Igneous rocks have also not been observed in the wells studied in this research. Furthermore, the magnetic anomaly map of the Netherlands, which is based on the presence of magnetic elements in for example magmatic rocks, does not show significant values in the study area (Appendix D). Therefore an igneous mound origin is discarded.

Salt

In the study area no salt structures pierce through the overlying layers up to Cenozoic sediments (fig.2). Furthermore wells in the study area do not show signs of evaporates at the MMU and therefore a salt lithology is not likely (fig.7 & table 3).

Carbonate

Carbonate mounds are generally related to a continuous flux of hydrocarbons seepage at the seafloor that act as nutrients for abnormal biological activity (Hovland & Judd, 1998). This leakage can result in local carbonate build-ups, such as bioherms e.g. reefs formed by corals or large communities of sponges (Dahlgren and Lindberg, 2005). The mounds would build out from a centered point and would result in downlapping internal reflections. This characteristic can be seen in the internally layered mounds (fig. 38). Another characteristic of carbonate mounds is a distinct seismic signature, due to the strong acoustic impedance contrast. This gives rise to strong amplitudes and velocity pull-ups. Velocity pull-ups can sometimes be seen beneath the mounds (fig. 38.1), but the strong amplitude response of the mounds compared with overlying sediments is absent (fig. 38.2).

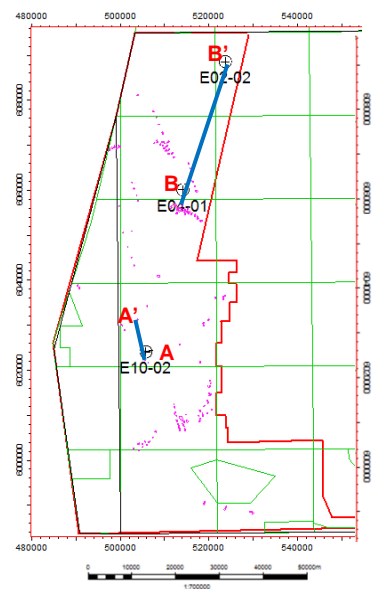
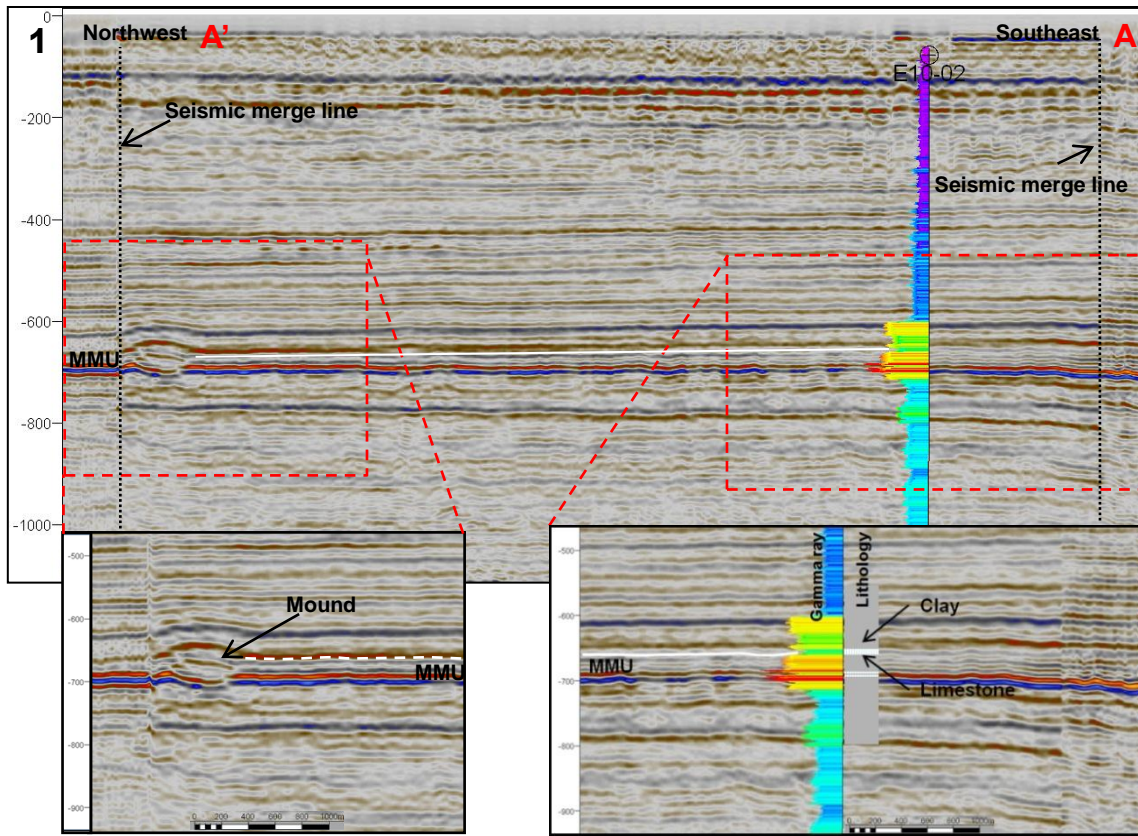
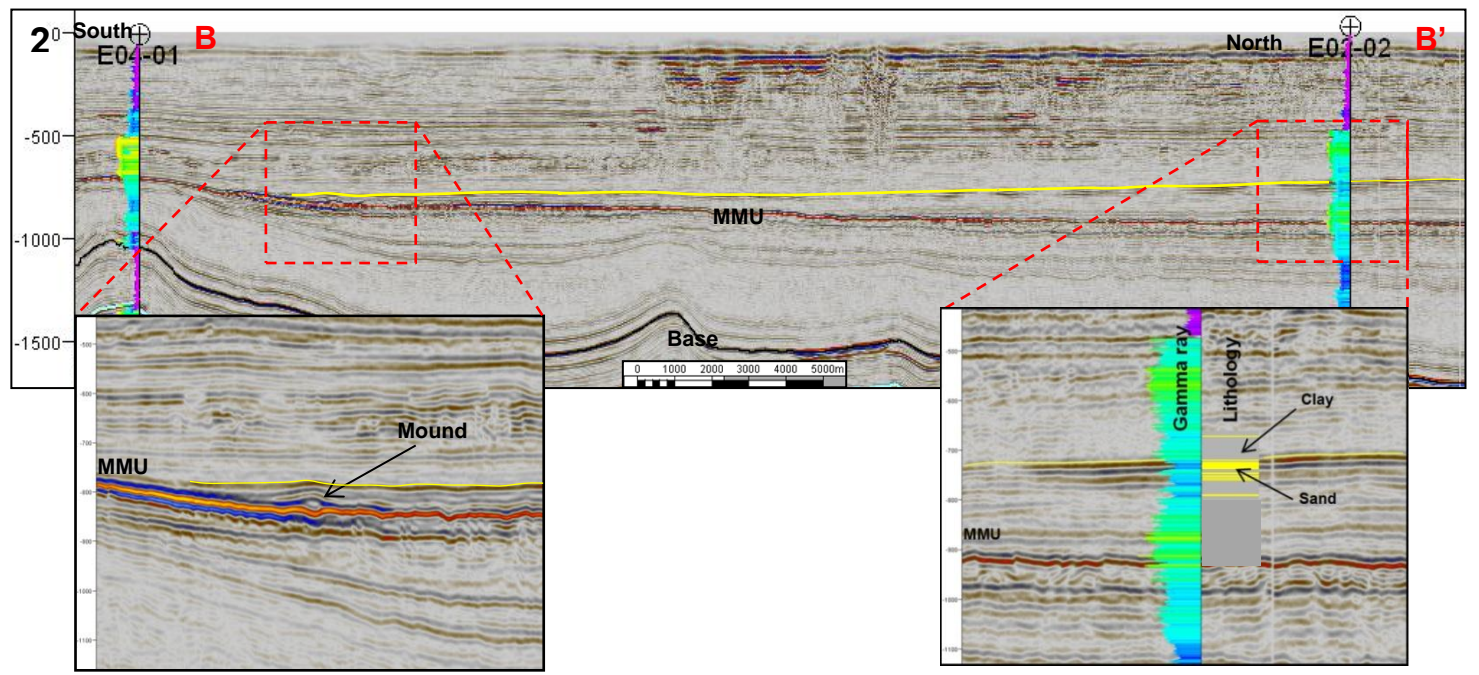


Fig.54) Two cross sections through the focus area as indicated on the map. A-A' shows the occurrence of a limestone layer at the MMU. B-B' shows the occurrence of a sand layer above the MMU.



Well E10-02 shows the presence of a limestone layer at and just above the Mid Miocene Unconformity (fig. 54.1 & table 3). This layer can be correlated on seismic cross section to a mound found in the northwest, which might indicate the lithology of the mounds to be carbonate. The question remains if this limestone layer represents a mound, as carbonate mounds do not appear as continuous reflectors in the subsurface but are rather recognized as distinct structural relief features.

The process of carbonate mound growth do not correspond with all characteristics observed regarding the mounds, therefore another origin is more likely in the study area.

Siliciclastic

Mound shaped siliciclastic features on the seafloor can be formed by different geological processes; cohesive gravity flow deposits (Jennette et al, 2000), contourites (Stow et al, 2001) and siliciclastic extrudites (Hansen et al, 2005; Hurst et al, 2006; Andresen et al 2009, 2010).

The process of cohesive gravity flow deposition e.g. turbidites and debrites, has been proposed for internally layered sandstone mounds in the UK Central Graben (Jennette et al, 2000).

However, in the study by Jennette et al (2000) these are related to channels and fan lobes. In this study these features have not been observed at the Mid Miocene Unconformity. Submarine landslides do however affect the MMU in the G-quadrants (Bardi, 2009 TNO), where similar mounded structures have been identified.

Contourites represent deposits formed under the influence of bottom parallel currents. These may be created by seafloor-erosion, creating depressions, and subsequent re-deposition of sediments next to these depressions (Stow et al, 2001). The mounds at the MMU in this study, are found on top of depressions rather than next to them. Furthermore, the mounds observed in this study do not show a dominant direction but rather align directing salt domes.

Since there seems to be a relation between the mounds and underlying polygonal faults in this study, it is unlikely that the processes of gravity flow deposition and contourites are able to explain the origin of the mounds.

Table.3) Lithology of the sediments at the MMU for the wells in the study area, based on composite well logs. Location of wells in fig.30

	Lithology
Well	Mid Miocene Horizon
D12-01	Clay
D12-04	Clay
D12-05	Clay
D15-02	Clay
D15-03	Clay
D18-01	Clay with minor sand and limestone
E02-01	Clay
E02-02	Clay
E04-01	Sand
E06-01	Clay
E10-01	Clay
E10-02	Limestone
E12-02	Clay
E12-03	Clay
E13-01	Clay
E14-01	Clay
E16-01	Clay
E16-02	Clay
E16-03	Clay
E17-01	Clay with minor sand
E17-02	Clay with minor sand
E18-02	Clay
E18-03	Clay
F02-03	Conglomerate of limestone and sandstone clasts in a clay matrix

The process of creating mounds via sand and mud extrusion e.g. subsurface sediment remobilization, requires fluid and/or hydrocarbon migration through unconsolidated sediments, entrain them and expel the mixture to the seafloor (Cartwright et al, 2007). This might also explain the relation between the structural relief and the throw of the underlying polygonal faults. Structural relief is larger in regions with larger throw values, which thus might have acted as source regions for the sediments. The observation of a smaller graben compared to the structural relief of the overlying mound, might be related to the relatively large source area of the Mid- and Lower North Sea group sediments resulting in a small depression on the Mid Miocene Unconformity (fig. 38.2) (Andresen et al, 2009).

Migration of fluids is visible on seismic data as distinct chaotic reflections, being characteristic for gas chimneys (Loseth et al, 2009) or pipe structures (Cartwright et al, 2007). Generally sand and mud extrusion on the seafloor is accompanied by an intrusive domain, which damages the primary internal layering. The intrusive domain can be identified on seismic cross sections (fig. 27) and in the study area a vertical disturbance beneath the mounds is observed only occasionally, indicating fluid migration pathways (fig.38.1). A possible explanation for the frequent absence of these disruptions might be due to the polygonal faulted sequence beneath the mounds. The polygonal faults might act as preferential pathways for fluids and/or sediments and prevent the internal layering to be further damaged.

Generally mud and sand extrusions are related to an external source of fluid and/or hydrocarbons mobilizing the sediments. The external sources represent fluids leaking from deeper levels through the overlying sedimentary sequences. Possible external sources could be the draining of Zechstein rafts e.g. anhydrite blocks from which overpressured fluids are released (Ligtenberg et al, 2005), or fluid and/or hydrocarbon leakage from deeper underlying reservoirs (Loseth et al, 2009). However, no indication of these structures is visible on seismic data underlying the mounds.

Another potential source of the fluids may be provided by the dewatering of the thick, underlying sequences of Middle- and Lower North Sea groups sediments. It is known from polygonal faulted section that this package has undergone extensive compaction and associated fluid expulsion. Polygonal faults tend to grow in size, in regions where fluids become focused (Berndt et al, 2003). It thus seems plausible that focused fluid flow is able to entrain and expel large volumes of sediment, in areas with the largest throw values e.g. mounded areas.

The distinction on the lithology of the mounds between mud and sand remains difficult. Well E2-02 shows the presence of sandstone layers from the Eridanos delta above the MMU. This layer can be correlated on seismic cross section to a mound found in the south (fig. 54.2 & Table 3). The other wells in the study area however generally show clay at the MMU, with the exception of the limestone in well E10-02.

If the mounds have been formed by sediment extrusion and are related to the underlying polygonal faults, the sediments originate from below. The wells studied in this research however, do not show the presence of sand in the Middle- and Lower North Sea groups. Therefore a sand lithology is difficult to prove. However, if the mounds have been formed by mud, these would have a similar lithology as surrounding sediments. But this contradicts with the observed velocity pull-up observed beneath the mounds (fig. 38.1 & 45), which is generally not associated with mud (Loseth et al, 2009).

Based on the observation on 3D seismic data, an origin of the mounds by siliciclastic sediment remobilization is thus considered the most likely. The mounds result from the dewatering of the Paleogene mudstones, which entrains the sediments in the ascending fluids and expel the fluid-sediment mixture at the paleo seabed. Additional data, such as wells drilled directly through one of the mounds, could help to identify the exact origin and lithology of the mounds

5.3 Implications for the petroleum industry

Fluid flow escape features can have various implications for hydrocarbon exploration and production (Huuse et al, 2010; Cartwright et al, 2007). This section will briefly discuss the implications of the mounded structures and polygonal fault system observed in this study for the petroleum industry.

If the mounded structures represent remobilized sediments, they are part of a linked intrusion-extrusion system (Huuse et al, 2010). Generally, remobilized sandstones show high porosity and permeability compared to the encasing sediments. Therefore remobilized sandstone systems can be volumetrically significant reservoirs; intrusive as well as extrusive (Hurst et al, 2006, 2007). However, there is no indication of the mounds being hydrocarbon filled sandstone reservoirs, as they do not show amplitude enhancements, which are characteristic for hydrocarbon occurrences. The increased porosity and permeability enables remobilized sandstones to act as migration pathways for ascending fluids and/or hydrocarbons, which might potentially fill overlying traps such as the shallow gas fields of the Upper North Sea group. If the mounds would resemble mudstone intrusions or extrusions, there is little change to the sediment porosity and permeability as the encasing sediments are composed of mudstones.

Remobilized sediments can also have negative influences. The intrusions pierce through overlying layers, thereby degrading the seal integrity. Furthermore, remobilized sediments are related to overpressure generation and may represent drilling hazards if these structures contain overpressured fluids.

Polygonal fault systems have been linked to dewatering and vertical fluid migration through fine grained sediments (Gay et al, 2004; Cartwright, 2011). These systems might also be exploited by remobilized sediment intrusions (Shoulders et al, 2007). Polygonal fault formation could therefore degrade the seal integrity of the fine grained sediment sequence, as well as be migration pathways for ascending fluids and/or hydrocarbons. The occurrence of bright spots in the Upper North Sea group (Schroot et al, 2003) might indicate the polygonal fault system acting as migration pathway for hydrocarbons ascending from the underlying Carboniferous source rock.

Based on these possible implications for the petroleum industry it is important to identify the polygonal fault system and mounded structures when drilling for hydrocarbon prospects. The structures are able to differentiate both the reservoir and sealing characteristics and give valuable information on the fluid flow dynamics present in the Dutch offshore.

6. Conclusion

This study aims to define the origin, composition and factors relating to the distribution of the mounded structures found on the Mid Miocene Unconformity. Another part of this research attempts to identify a possible relationship with the underlying polygonal fault system via quantitative analysis on the mounds and polygonal faults.

In total, 135 mounded structures have been identified on the Mid Miocene Unconformity in the study area, which is located in D- and western E quadrants of the northern Dutch offshore. The mounds have generally been found in the vicinity of salt domes on the Cleaverbank- and Silverpit platform.

The polygonal fault system present in the northern Dutch offshore has only been recognized in the Paleogene sequence and terminates at the Mid Miocene Unconformity. This observation corresponds with the polygonal fault system present in the Central North Sea (Cartwright et al, 1994).

- Based on the quantitative analysis on the polygonal faults measurements of azimuth and fault trace length values do not show significant differences between areas with mounds or without. Therefore a predictable relationship between the polygonal faults and overlying mounded structures is difficult to establish for these fault characteristics.
- A predictable relationship has been observed between the polygonal faults at the Mid Miocene Unconformity and overlying mounded structures for the measured throw values. The areas where the polygonal fault throw is largest, generally coincide with the occurrence of mounds. Furthermore a positive relation has been observed between the structural relief of the mounds and the magnitude of the underlying fault throws, suggesting a genetic relation between both features.
- The most likely interpretation of the mounds is that these originate as clastic remobilized sediments. Fluids dewatering from the underlying polygonal faulted sequence resulted in the entrainment and expulsion of the sediments on the paleo seafloor. However, additional data is needed to identify the exact origin and lithology of the mounds.
- Implications for the petroleum industry comprise a possible degradation of the sealing capacity for the Paleogene mudstones of the Middle- and Lower North Sea group, since the polygonal fault system and mounds can act as vertical fluid migration pathways. Furthermore, the mounds potentially represent drilling hazards if they contain overpressured fluids.

7. Recommendations

Although the Dutch offshore is a well explored area, fluid flow expressions continue to be recognized. These fluid expressions give valuable information on the fluid flow processes present in the Southern North Sea region and could have various implications for the petroleum industry.

This research focused on the mounded structures recognized on the Mid Miocene Unconformity, but many other fluid flow expressions have been identified. These additional observations are combined in Appendix D and can be used to further explore and understand the geological fluid flow processes present in the Dutch subsurface.

The polygonal faulted sequence recognized in this research has only been used to identify a possible relationship with the overlying mounded structures. However, the mechanism responsible for the polygonal fault system has not been investigated. The availability of new, high resolution 3D seismic data in the northern Dutch offshore might be used to identify the mechanism responsible for the genesis of the polygonal fault system.

8. Acknowledgements

First of all I would like to thank Guido Hoetz and Mijke van den Boogaard for giving me the opportunity to do my master thesis at EBN in Utrecht. Their guidance and advice throughout my time at EBN enabled me to construct this report. I also would like to thank the technical department of EBN for their helpful discussions and ideas. Bastiaan Jaarsma, for reviewing and his guidance with the Petrel software. Hans de Bresser, my supervisor from the UU, is thanked for his reviewing sessions, ideas and comments. Ide van der Molen from NAM, and Geert de Bruin from TNO, are thanked for their ideas. Finally, I would like to thank my fellow “thesis writers” from the 3rd floor at the Earth Science building, Richard Wessels, Michiel Koolschijn, Eddy Wally and Jort Koopmans, for their helpful discussions and feedback.

